Supplementary Information

Monitoring ADP and ATP in Vivo Using a Fluorescent Ga(III)−Probe Complex

Xinyu Zhang, Yuqian Jiang and Nao Xiao*

Beijing Area Major Laboratory of Peptide and Small Molecular Drugs, Engineering Research Center of Endogenous Prophylactic of Ministry of Education of China, School of Pharmaceutical Sciences, Capital Medical University, Beijing, 100069, China

E-mail: xiaonao@ccmu.edu.cn

General considerations. All analytical and spectroscopic grade chemicals were used from commercial sources unless specifically stated. Ultrapure water was used throughout the experiments. UV-vis absorption spectra were recorded at 25 °C using a SHIMADZU UV-2550 spectrophotometer. Fluorescence spectra were recorded using a HITACHIF-2500 fluorescence spectrometer with a xenon discharge lamp in 1 cm quartz cells with a slit width of 2.5 nm. All measurements were performed at room temperature. ^{1}H NMR (300 MHz) and ^{13}C NMR (75 MHz) spectra were recorded on Varian INOVA-300 MHz spectrometer, and chemical shifts (δ) were reported as ppm with tetramethylsilane (TMS) as the internal standard. ESI/MS spectra were recorded on ZQ 2000 (Waters, US) and solariX FT-ICR mass spectrometer (Bruker Daltonik) with an ESI/MALDI dual ion source and 9.4 T superconductive magnet, by infusing samples directly into the source at 20 μL/min using a syringe pump. The spray voltage was set at 4.7 kV and the capillary temperature at 70 °C. Fluorescence lifetimes were detected by a FLS980 fluorescence spectrometer from Edinburgh Instruments. The monitored wavelength was 518 nm. The fitting parameters (decay times and pre-exponential factors) were decided by minimizing the reduced chisquare χ^2. Quantum yields (Φ) were determined at room temperature. The excitation light (440 nm) from an Edinburgh Instruments FLS980 spectrometer was used as the irradiation light source. Cellular uptake and distribution of L-Ga^{3+} and ATP were observed by TCS SP5 confocal microscopy (Leica Microsystems, Wetzlar, Germany). The adult zebrafish were imaged using an IVIS Imaging System. The single crystals of **L** suitable for X-ray analysis were grown in DMSO-d_6-D_2O. Data collections were performed at 180 K using graphite-monochromated Mo Kα radiation (λ = 0.71073 Å) on a XtaLAB Pro: Kappa single diffractometer. Crystallographic data (CCDC 1848345) has been deposited with the Cambridge Crystallographic Data Centre as supplementary publication nos.

Synthesis of (*E*)-1-((2-(benzo[*d*]thiazol-2-yl)hydrazono)methyl)naphthalen-2-ol (L)

L was synthesized according to previously reported method[1, 2] with some modifications. 2-Hydrazinobenzothiazole (172.18 mg, 1.0 mmol, 200 mL) was mixed with 2-hydroxy-1-naphthaldehyde (165.21 mg, 1.0 mmol, 200 mL) in absolute methanol, which was refluxed for about 2 h. The resulting yellow colored product was filtered and washed with cold ethanol and dried in vacuo. Yield: 284.89 mg (89.20%). ^{1}H NMR (DMSO-d_6/D_2O, δ/ppm): 9.17 (s, 1H, NH), 8.58 (s, 1H, HC=N), 7.88 (t, *J*=17.1 Hz, 3H, Ar and Bt), 7.73 (d, *J*=7.2 Hz, 1H, Ar), 7.58 (t, *J*=14.4 Hz, 1H, Ar), 7.40 (t, *J*=15.0 Hz, 1H, Ar), 7.32 (d, *J*=6.0 Hz, 2H, Bt), 7.23 (d, *J*=9.0 Hz, 1H, Ar), 7.11 (t, *J*=12.6 Hz, 1H, Ar). ^{13}C NMR (DMSO-d_6, δ/ppm): 166.33, 157.44, 132.84, 131.73, 129.29, 128.48, 128.25, 127.03, 124.06, 122.56, 122.26, 118.73, 109.96. ESI-MS (*m*/*z*): 318.38 $[M-H]^-$ (Calcd. for $C_{18}H_{12}N_3OS$: 318.07).

Sample preparation and measurements

Stock solutions of LiCl, $NaSO_4$, $MgSO_4$, $AlCl_3$, KNO_3, $CaCl_2$, $CrCl_3$, $BaCl_2$, $MnCl_2$, $FeSO_4$, $Fe_2(SO_4)_3$, $CoCl_2$, $Co(NH_3)_6Cl_3$, $NiCl_2$, $CuSO_4$, $Zn(ClO_4)_2$, $Ga(NO_3)_3$, $CdCl_2$, $InCl_3$, $BaCl_2$ and $Ce(NO_3)_3$ were prepared in deionized water, and concentrations of the metal ions were fixed to 2.0×10^{-2} M. These solutions were used to provide metal ions in related experiments. Stock solutions of TBAI (tetrabutylammonium iodide), TBAF (tetrabutylammonium fluoride), TBABr (tetrabutylammonium bromide), TBACl (tetrabutylammonium chloride), TBACN (tetrabutylammonium cyanide), ATP (adenosine 5'-triphosphate), KNO_3, Na_2CO_3, K_2SO_4, Na_3PO_4, $Zn(ClO_4)_2$, $NaHCO_3$, $NaHSO_4$, NaH_2PO_4 and $Ni(CH_3COO)_2$ were prepared in deionized water, and concentrations of the anions were fixed to 2.0×10^{-2} M. These solutions were used to provide anions in related experiments. Stock solution of **L** (1.0×10^{-3} M) was prepared in DMSO–H_2O (v/v = 9:1) solution. In a typical titration experiment, the host solution was transferred to a fluorescence cell and then further diluted to 5.0×10^{-6} M in 2.0 mL volume for titration experiments. The emission spectrum was recorded at 518 nm under room temperature. The guest solution was added through a micropipettor to the host solution, and the amount was increased until 10 equiv. of the guest. The fluorescence spectrum of each solution was recorded after each addition. Every time an appropriate volume of each analyte was added to the test solution.

Evaluation of the Cell Viability and Metabolic Activity

The survival rates of cells administered with Ga^{3+}, **L** and L-Ga^{3+} were determined by a standard 3-(4,5-dimethylthiazolyl-2)-2,5-diphenyltetrazolium bromide (MTT) analysis. In brief, the normal human bronchial epithelial (16HBE) cells were seeded in a 96-well microplate and cultured with Ga^{3+}, **L** or L-Ga^{3+} at various concentrations, supplemented with 10% (*v*/*v*) fetal bovine serum, 1% antibiotics, and cultured at 37 °C in an atmosphere of 5% CO_2. Meanwhile, the cells treated with medium only were used as control. Then, the 20 μL of 0.5 mg/mL MTT solution was added into each well for 4 h. The incubation was suspended by removing the medium and adding 100 μL of DMSO. After a 15-min gentle vortex, the light absorption value of each well was recorded at 490 nm on an Infinite M 200 Pro Multilabel Plate Reader (Tecan, Mannedorf, Switzerland).

Fluorescence imaging of cellular uptake of L-Ga^{3+}

The chemosensor L-Ga^{3+} (60.0 μM) in the culture medium was prepared by diluting it (1.0 mM) in DMSO–H_2O (v/v = 9:1) solution. The ADP or ATP (120.0 μM) in culture medium was prepared by diluting it (1.0 mM) in distilled water. Normal human bronchial epithelial (16HBE) cells were incubated on 35 mm glass-bottomed cell culture dishes with L-Ga^{3+} (60 μM), supplemented with culture medium at 37 °C for 1 h in a humidified incubator with 5% CO_2 and 20% O_2. After removing culture, the cells were rinsed slightly 3 times with fresh culture medium.

The cell nuclei were then stained with Hoechst 33342 in culture medium (10 mg / mL) for 10 min. After washing with fresh culture medium, the cells treated with ADP or ATP were further incubated in fresh culture medium for 1 h. After staining, cells were then analyzed by Laser Scanning Confocal Microscope. The following wavelengths were used: excitation at 346 nm and detection through a 460 nm filter for Hoechst 33342, and excitation at 440 nm and detection through a 518 nm filter for L-Ga^{3+}.

Fluorescence imaging of L-Ga^{3+} and ADP or ATP in zebrafish

The adult zebrafish were obtained from local fish market in Beijing. For fluorescence imaging of L-Ga^{3+} in zebrafish, the zebrafish and L-Ga^{3+} (60 μM) in ultrapure water were incubated at room temperature for 1 h. After incubation, the water containing L-Ga^{3+} was removed, and the zebrafish was washed with water for three times before subjecting to fluorescence imaging using an IVIS Imaging System (Caliper) under excitation at 430 nm and emission at 520 nm band pass 30 wavelength filter. For analysis of ADP or ATP in adult zebrafish, the fish was supplied with ADP or ATP (120 μM) in water. After 1 h incubation, the zebrafish was treated with fresh water containing L-Ga^{3+} (60 μM) for 1 h. The fish was rinsed with water for three times before subjecting to fluorescence imaging.

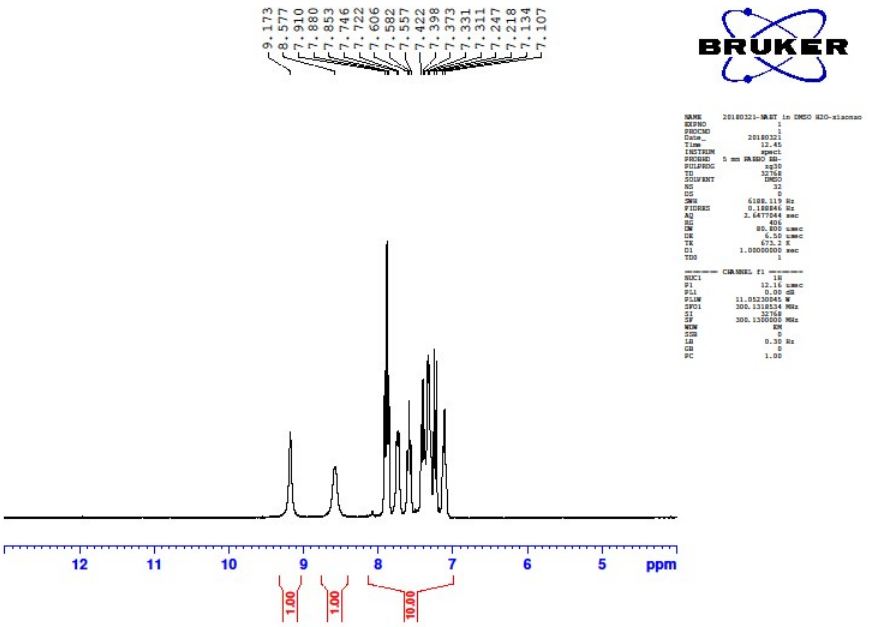

Fig. S1. ^{1}H-NMR spectrum of **L** in DMSO-d_6/D_2O.

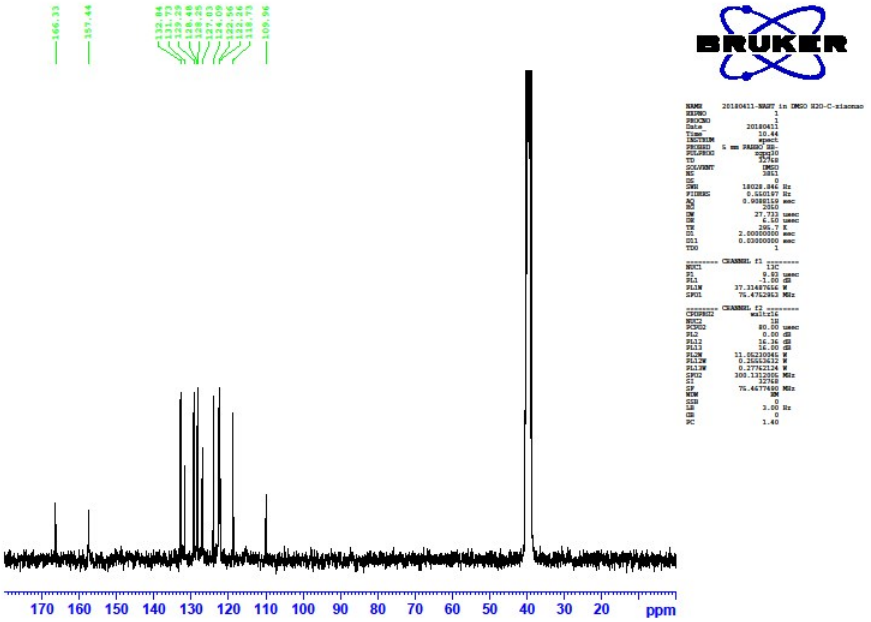

Fig. S2. ^{13}C-NMR spectrum of **L** in DMSO-d_6/D_2O.

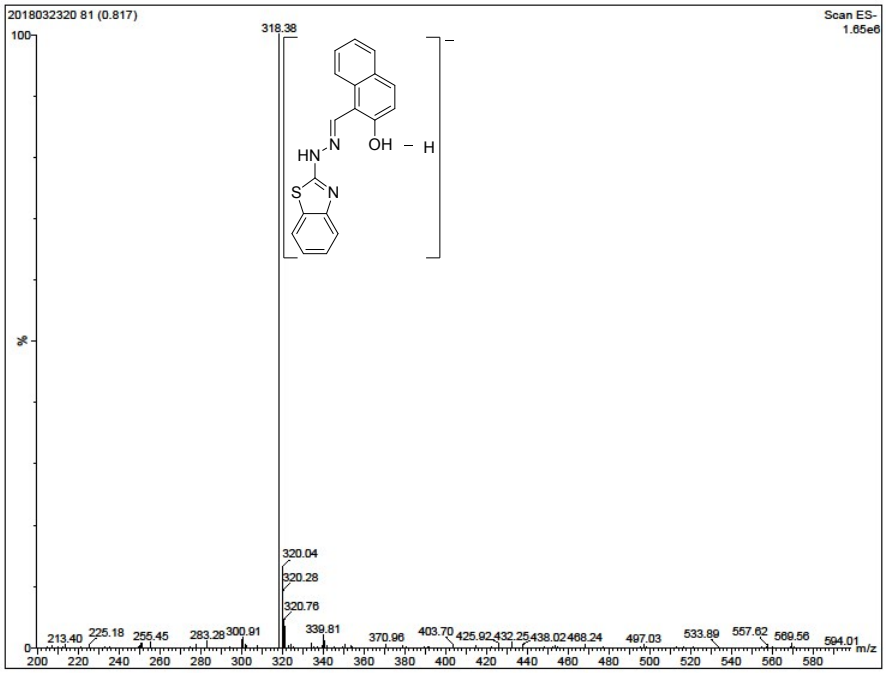

Fig. S3. The ESI-MS spectrum of **L** in negative mode. ESI-MS (*m*/*z*): 318.38 [**L**-H]$^-$ (Calcd. for $C_{18}H_{12}N_3OS$: 318.07).

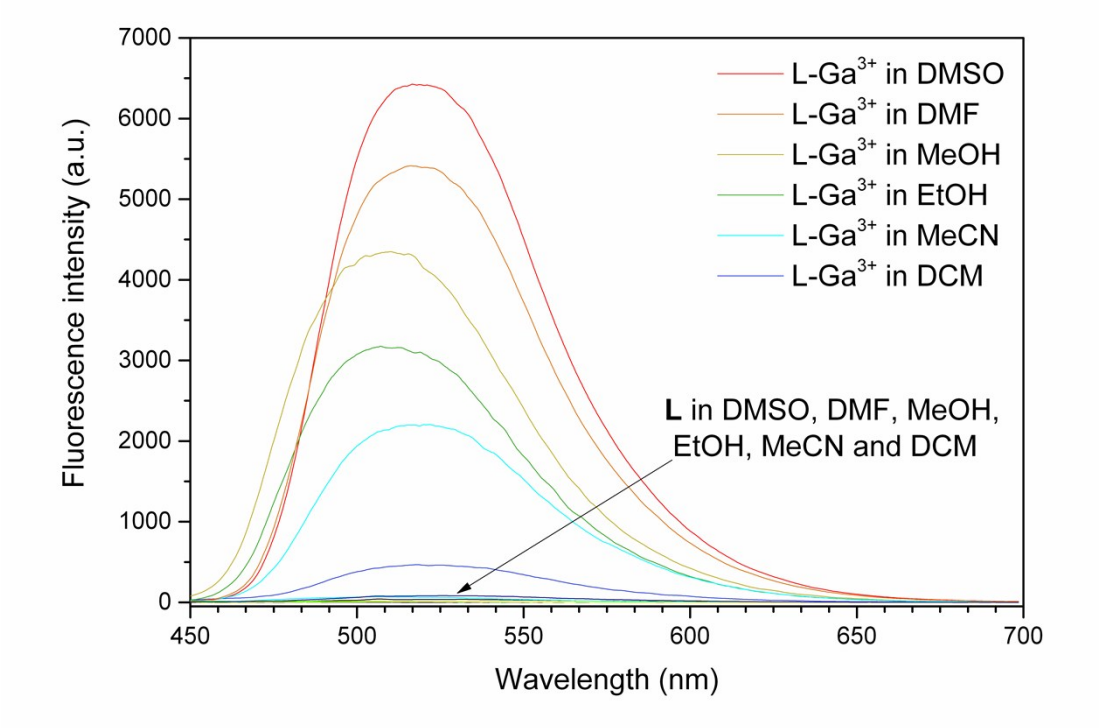

Fig. S4. Fluorescence responses of **L** (5.0 μM) and L-Ga^{3+} (5.0 μM) in various solvents (λ_{ex} = 440 nm).

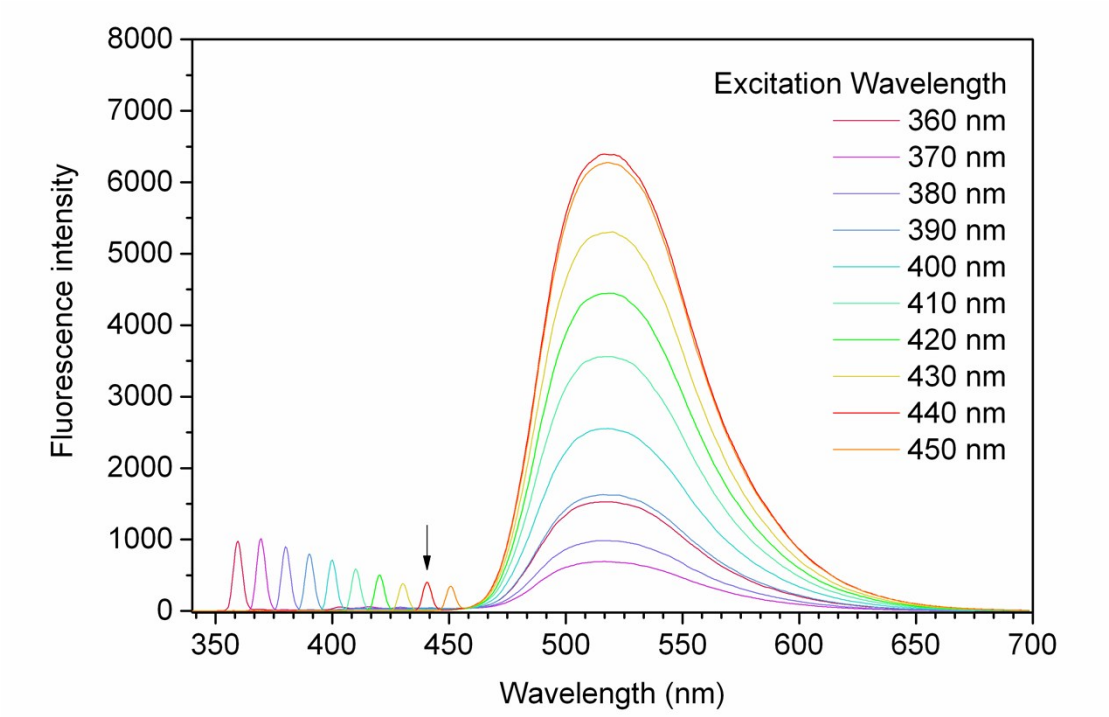

Fig. S5. Fluorescence spectra of L-Ga^{3+} (5.0 μM, DMSO) excited at a particular wavelength ranging from 360 nm to 450 nm. The highest fluorescence emission intensity, indicated in red, was obtained when a wavelength of 440 nm was used for excitation.

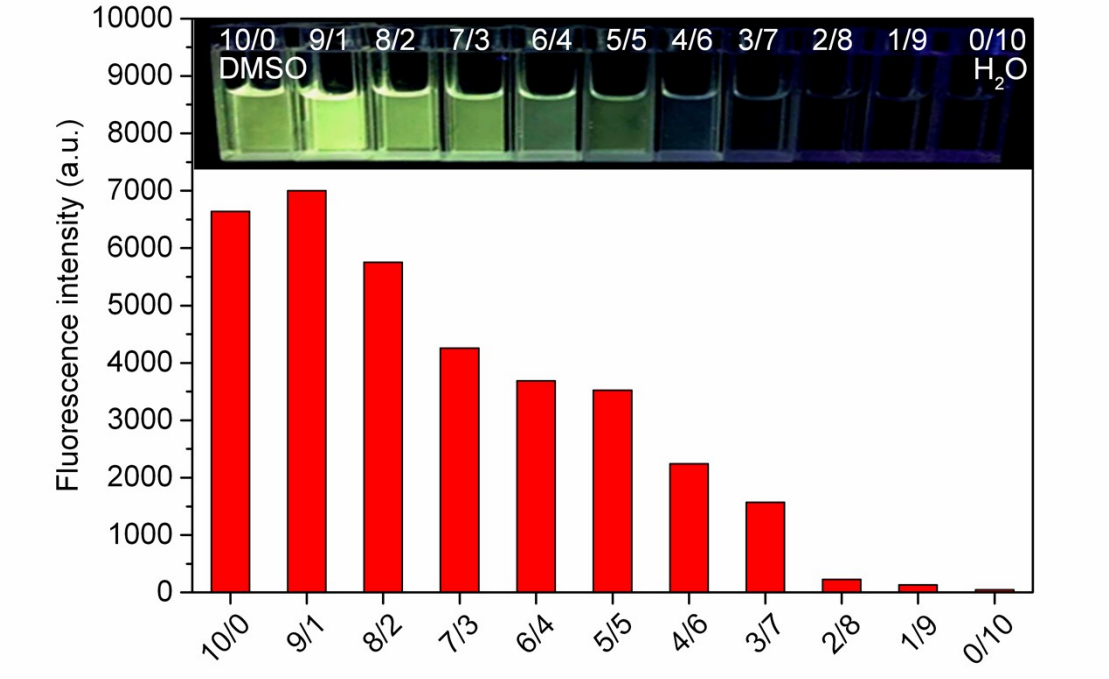

Fig. S6. The fluorescence responses of **L** (5.0 μM) to Ga^{3+} (50.0 μM) in various ratios of DMSO/H_2O (λ_{ex} = 440 nm). The ratios of DMSO/H_2O from left to right are 10/0, 9/1, 8/2, 7/3, 6/4, 5/5, 4/6, 3/7, 2/8, 1/9, and 0/10, respectively. Inset shows the fluorescent photographs of L-Ga^{3+} (5.0 μM) in DMSO/H_2O mixtures under 365 nm excitation.

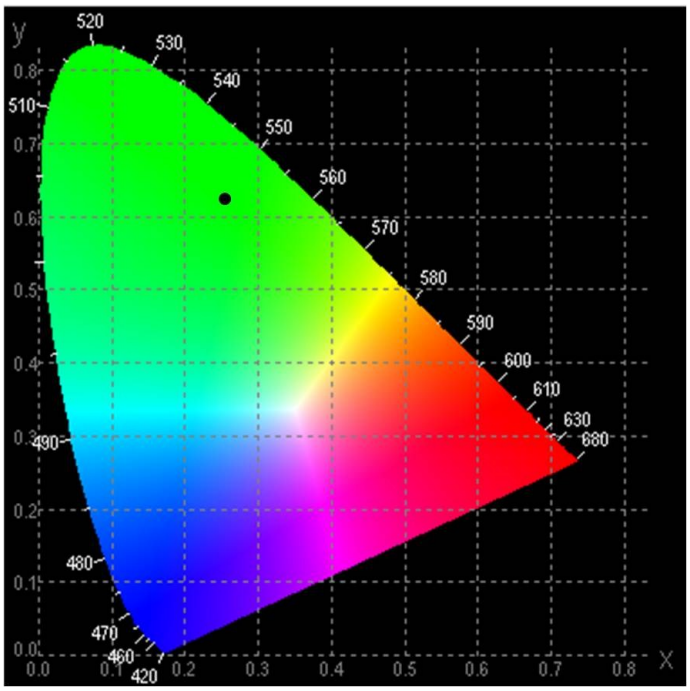

Fig. S7. The CIE (1931) chromaticity diagram for L-Ga^{3+} in DMSO/H_2O (*v*/*v* = 9/1) solution (λ_{ex} = 440 nm).

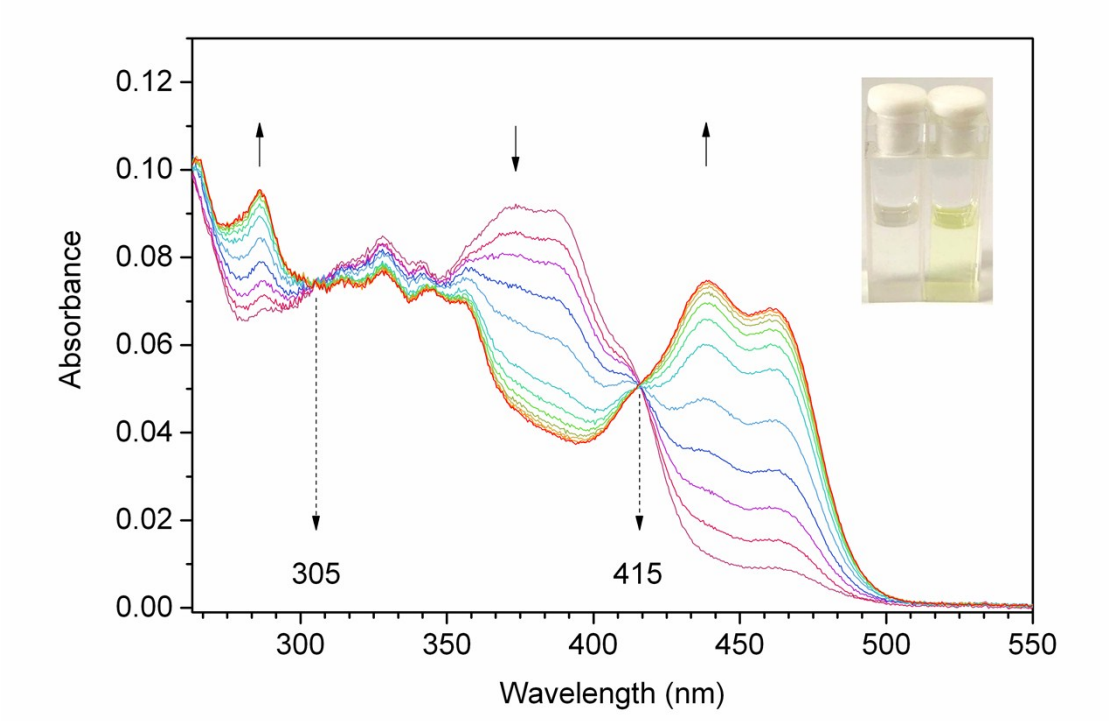

Fig. S8. The UV–vis spectra of **L** (5.0 μM) changes with addition of Ga^{3+} from 0 to 10.0 μM in DMSO/H_2O (*v*/*v* = 9/1) solution at room temperature.

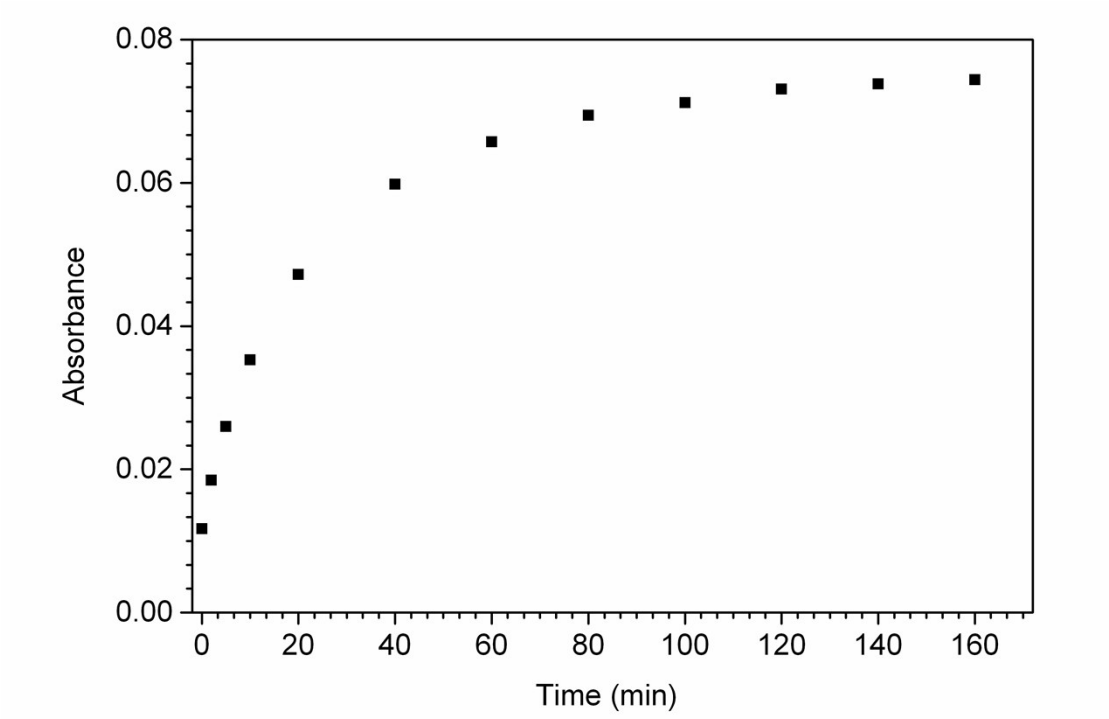

Fig. S9. Time-trace plots of the UV–vis absorbance of **L** (5.0 μM) at 440 nm in DMSO/H_2O (*v*/*v* = 9/1) solution. [Ga^{3+}] = 50.0 μM.

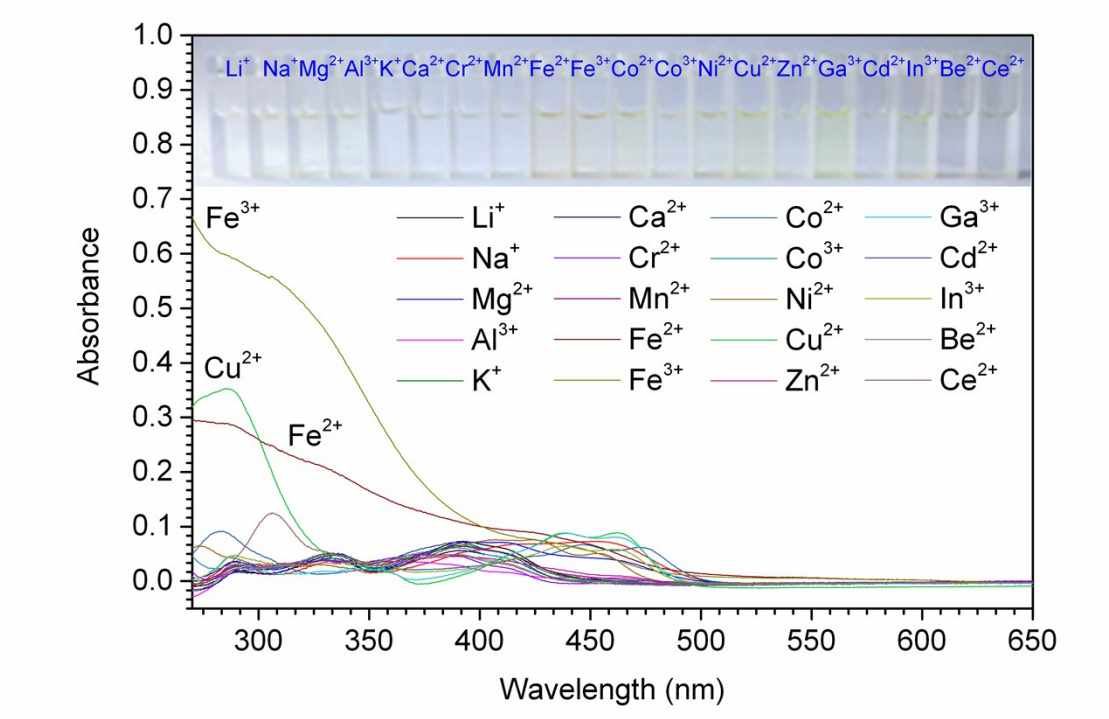

Fig. S10. UV-vis spectra of **L** (5.0 μM) with 10 equiv. of various metal ions in DMSO/H_2O (*v*/*v* = 9/1) solution.

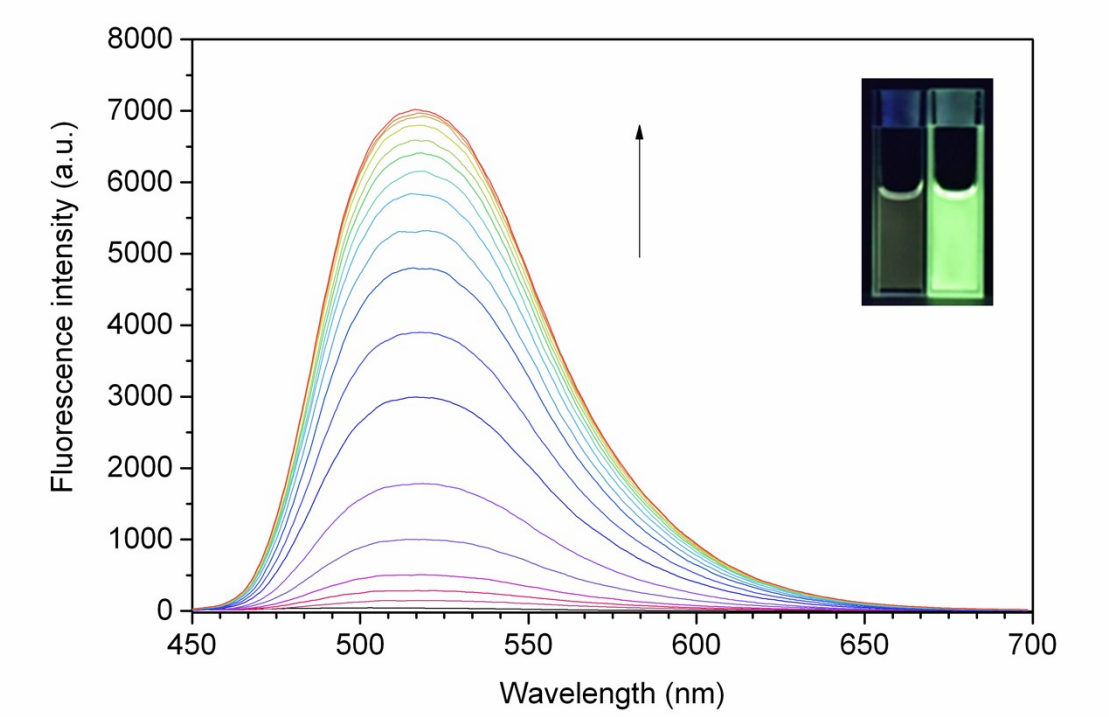

Fig. S11. Fluorescent spectra of **L** (5.0 μM) upon titration with Ga^{3+} from 0 to 10.0 μM in DMSO/H_2O (v/v = 9/1) solution at room temperature. λ_{ex} = 440 nm.

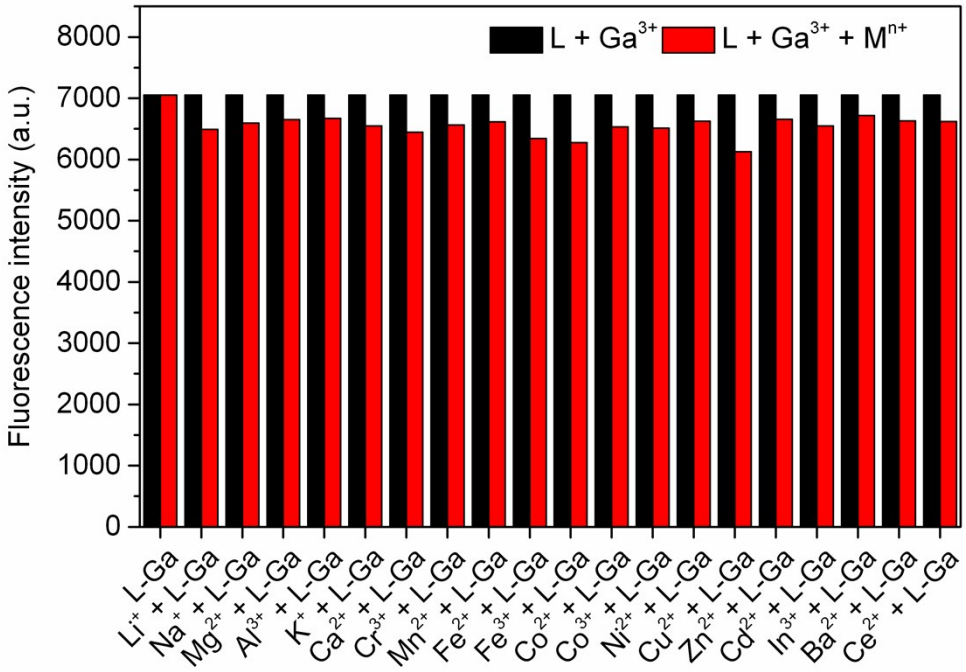

Fig. S12. Fluorescence responses of **L** (5 μM) to various metal ions (50.0 μM), and upon the subsequent addition of Ga^{3+} (50.0 μM) (λ_{ex} = 440 nm, λ_{em} = 518 nm). The response of **L** was included as controls. Left to right: **L** alone and **L** + M + Ga^{3+} (M = Li^+, Na^+, Mg^{2+}, Al^{3+}, K^+, Ca^{2+}, Cr^{3+}, Mn^{2+}, Fe^{2+}, Fe^{3+}, Co^{2+}, Co^{3+}, Ni^{2+}, Cu^{2+}, Zn^{2+}, Cd^{2+}, In^{3+}, Ba^{2+} and Ce^{2+}).

Table S1. Photophysical properties of **L** (5.0 μM) in the absence and presence of Ga^{3+} were recorded in DMSO/H_2O (*v*/*v* = 9/1) solution at room temperature. Decay times τ_1, τ_2 and average life time τ_A were presented in the table.

Addition of Ga^{3+}/μM	τ_1/ns	τ_2/ns	τ_A/ns	χ^2
0.0	0.51 (6.26%)	4.40 (93.74%)	4.16	1.070
Addition of Ga^{3+}/μM	τ/ns			χ^2
2.5	4.34			1.044
5.0	4.37			1.042
10.0	4.35			1.106
20.0	4.35			1.042
40.0	4.36			1.117

Table S2. Fluorescence quantum yield data of **L** (5.0 μM) in addition of various equivalents (0.5, 1.0, 2.0, 4.0 and 8.0) of Ga^{3+} were recorded in DMSO/H_2O (v/v = 9/1) solution at room temperature.

Compounds	ϕ
L + 0.5 Ga^{3+}	0.3546
L + 1.0 Ga^{3+}	0.6093
L + 2.0 Ga^{3+}	0.8920
L + 4.0 Ga^{3+}	0.8590
L + 8.0 Ga^{3+}	0.8271

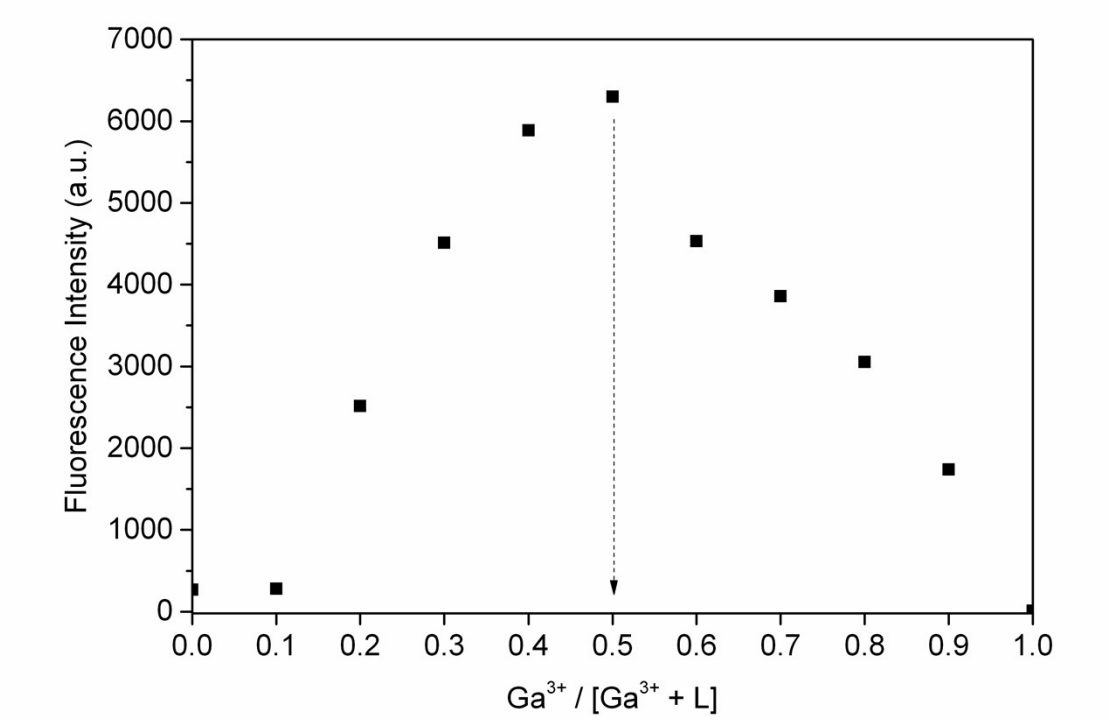

Fig. S13. Job's plot of receptor **L** and Ga^{3+}, where the intensity at 518 nm was plotted against the mole fraction of Ga^{3+}. The total concentration of Ga^{3+} ions with receptor **L** was 20.0 μM.

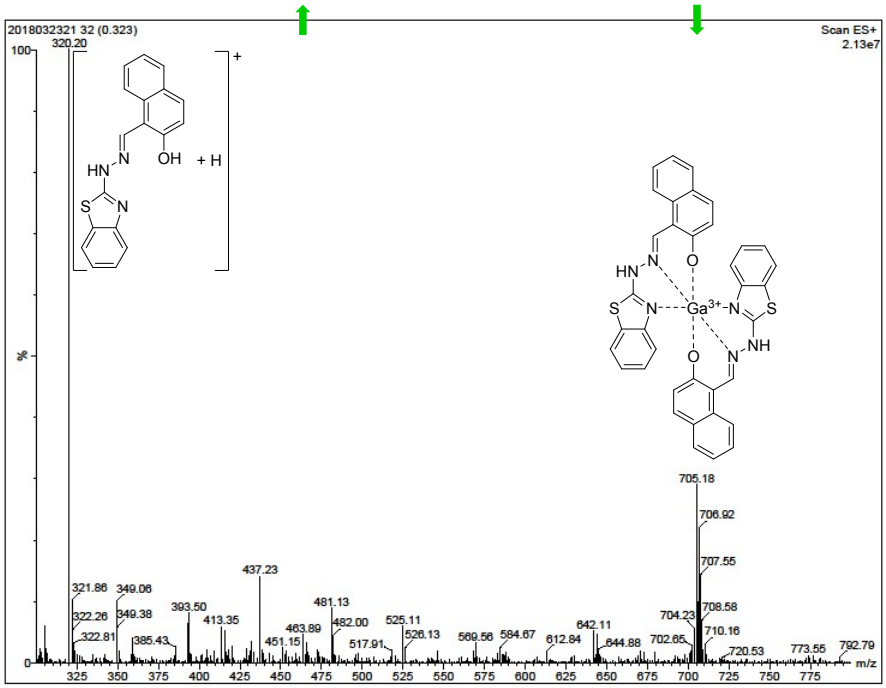

Fig. S14. The ESI-MS spectrum of **L** upon addition of 0.25 equiv. of $Ga(NO_3)_3 \cdot H_2O$ in positive mode. ESI-MS (*m*/*z*): 320.20 $[\mathbf{L} + H]^+$ (Calcd. for $C_{18}H_{14}N_3OS$: 320.09). ESI-MS (*m*/*z*): 705.18 $[2\mathbf{L} - 2H + Ga^{3+}]^+$ (Calcd. for $C_{36}H_{24}GaN_6O_2S_2$: 705.06).

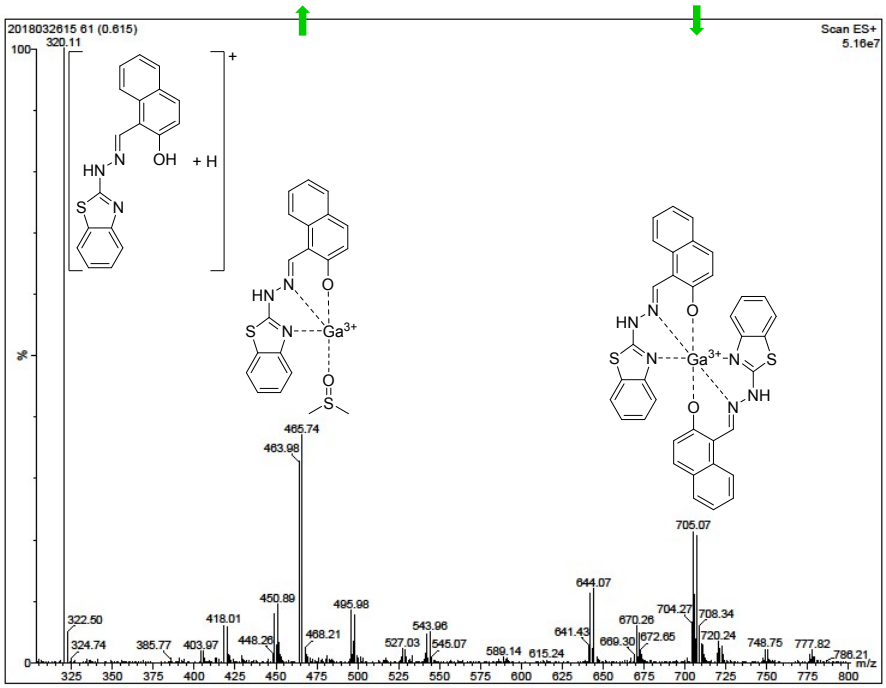

Fig. S15. The ESI-MS spectrum of **L** upon addition of 0.5 equiv. of $Ga(NO_3)_3 \cdot H_2O$ in positive mode. ESI-MS (*m*/*z*): 320.11 $[\mathbf{L} + H]^+$ (Calcd. for $C_{18}H_{14}N_3OS$: 320.09). ESI-MS (*m*/*z*): 465.74 $[\mathbf{L} - H + DMSO]^+$ (Calcd. for $C_{20}H_{19}GaN_3O_2S_2$: 466.02). ESI-MS (*m*/*z*): 705.07 $[2\mathbf{L} - 2H + Ga^{3+}]^+$ (Calcd. for $C_{36}H_{24}GaN_6O_2S_2$: 705.06).

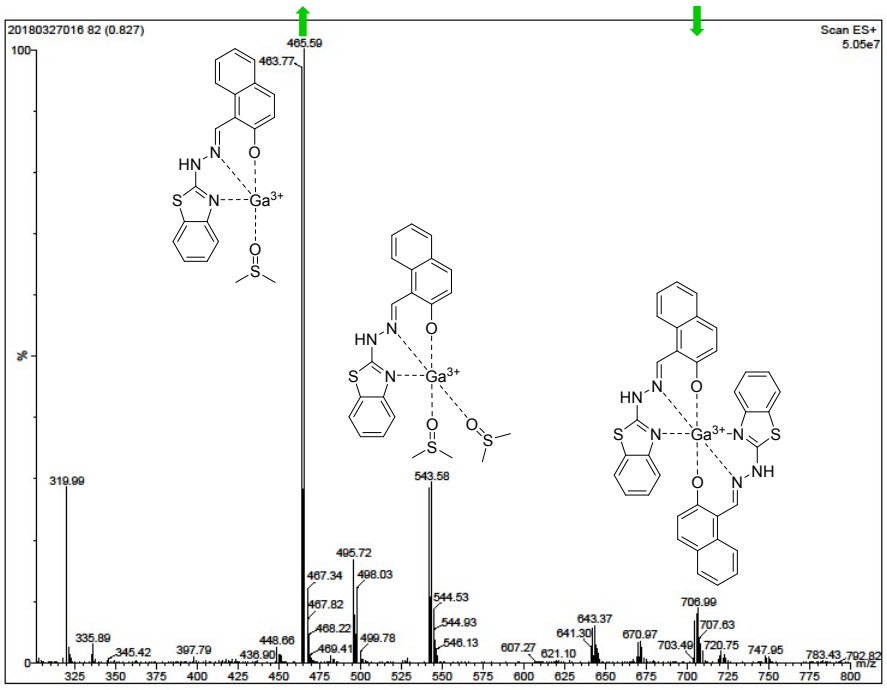

Fig. S16. The ESI-MS spectrum of **L** upon addition of 1.0 equiv. of $Ga(NO_3)_3 \cdot H_2O$ in positive mode. ESI-MS (*m*/*z*): 465.59 [**L** - H + DMSO]$^+$ (Calcd. for $C_{20}H_{19}GaN_3O_2S_2$: 466.02). ESI-MS (*m*/*z*): 543.58 [**L** - H + 2DMSO]$^+$ (Calcd. for $C_{22}H_{24}GaN_3O_3S_3$: 543.02). ESI-MS (*m*/*z*): 706.99 [2**L** - 2H + Ga^{3+}]$^+$ (Calcd. for $C_{36}H_{24}GaN_6O_2S_2$: 705.06).

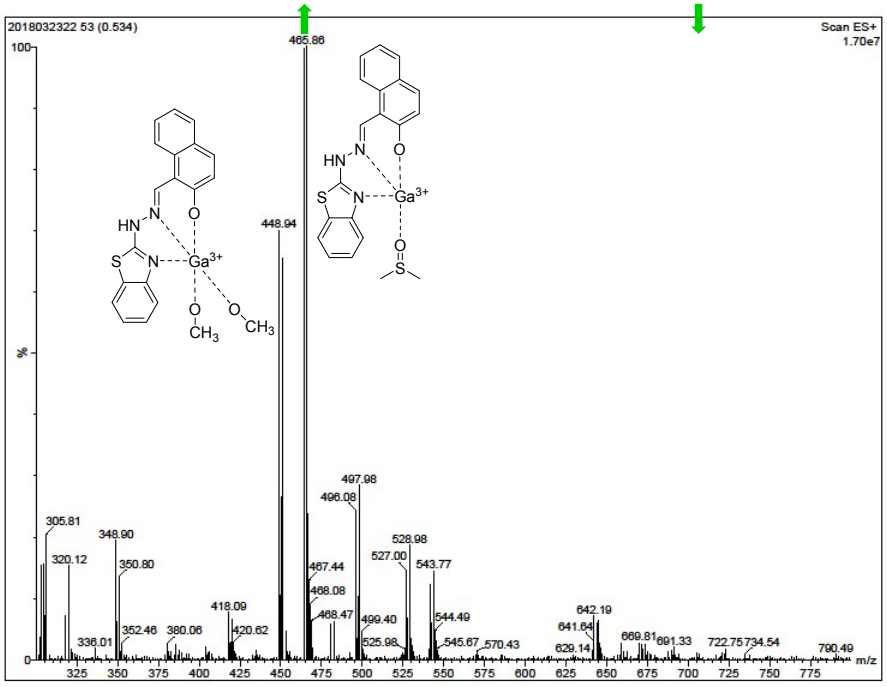

Fig. S17. The ESI-MS spectrum of **L** upon addition of 2.0 equiv. of $Ga(NO_3)_3 \cdot H_2O$ in positive mode. ESI-MS (*m*/*z*): 448.94 [**L** - H + 2MeOH - 2H]$^+$ (Calcd. for $C_{20}H_{18}GaN_3O_3S$: 449.03). ESI-MS (*m*/*z*): 465.86 [**L** - H + DMSO]$^+$ (Calcd. for $C_{20}H_{19}GaN_3O_2S_2$: 466.02).

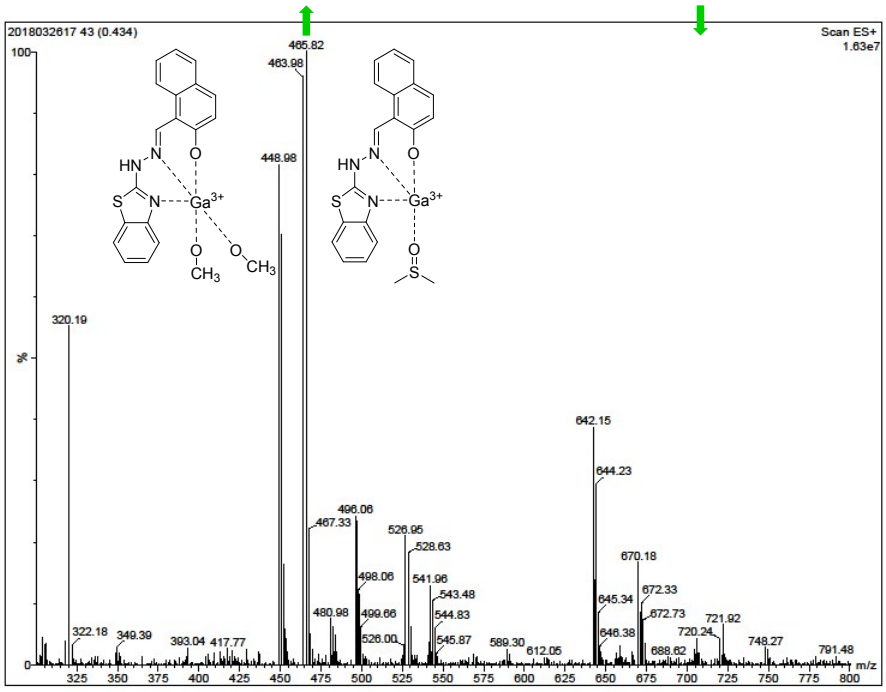

Fig. S18. The ESI-MS spectrum of **L** upon addition of 4.0 equiv. of $Ga(NO_3)_3 \cdot H_2O$ in positive mode. ESI-MS (*m*/*z*): 448.98 [**L** - H + 2MeOH - 2H]$^+$ (Calcd. for $C_{20}H_{18}GaN_3O_3S$: 449.03). ESI-MS (*m*/*z*): 465.82 [**L** - H + DMSO]$^+$ (Calcd. for $C_{20}H_{19}GaN_3O_2S_2$: 466.02).

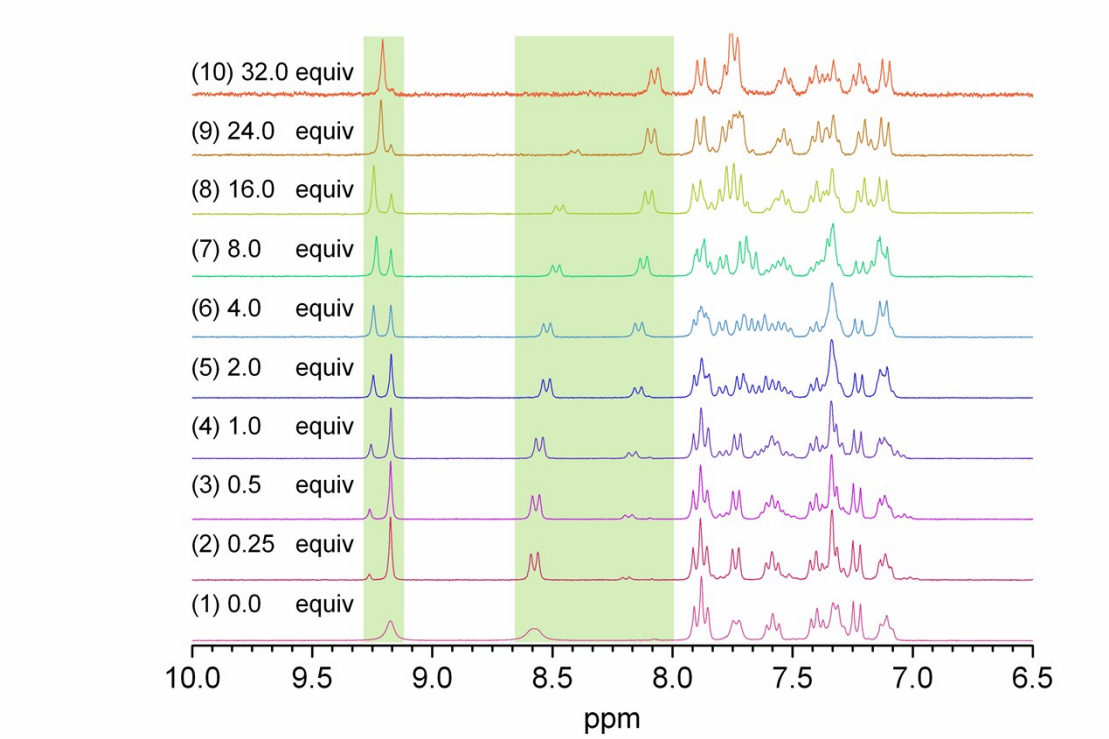

Fig. S19. ^{1}H NMR spectra of **L** in DMSO-d_6/D_2O solution upon addition of Ga^{3+} at room temperature: (1) **L** alone, (2) **L** with 0.25 equiv. of Ga^{3+}, (3) **L** with 0.5 equiv. of Ga^{3+}, (4) **L** with 1.0 equiv. of Ga^{3+}, (5) **L** with 2.0 equiv. of Ga^{3+}, (6) **L** with 4.0 equiv. of Ga^{3+}, (7) **L** with 8.0 equiv. of Ga^{3+}, (8) **L** with 16.0 equiv. of Ga^{3+}, (9) **L** with 24.0 equiv. of Ga^{3+} and (10) **L** with 32.0 equiv. of Ga^{3+}.

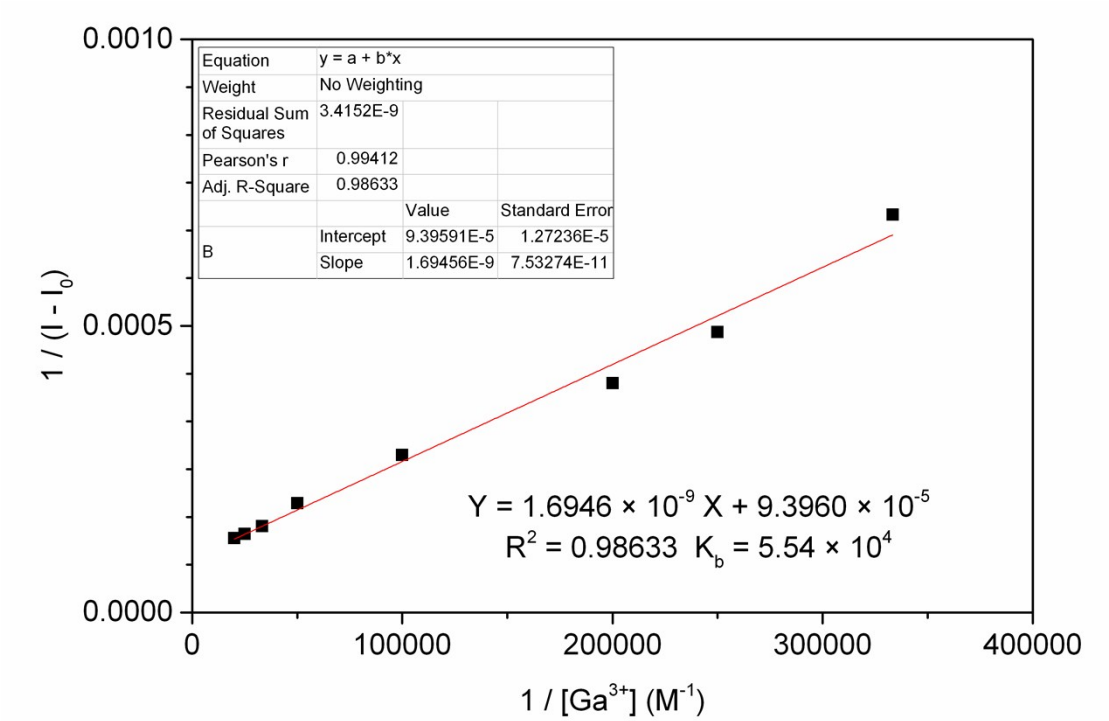

Fig. S20. Benesi-Hildebrand plot of **L** (λ_{em} = 518 nm), assuming 1:1 stoichiometry for association between **L** and Ga^{3+} in DMSO/H_2O (v/v = 9/1) solution.

$$\frac{1}{\Delta F} = \frac{1}{\Delta F_{\max}} + \left(\frac{1}{K[C]}\right)\left(\frac{1}{\Delta F_{\max}}\right)$$

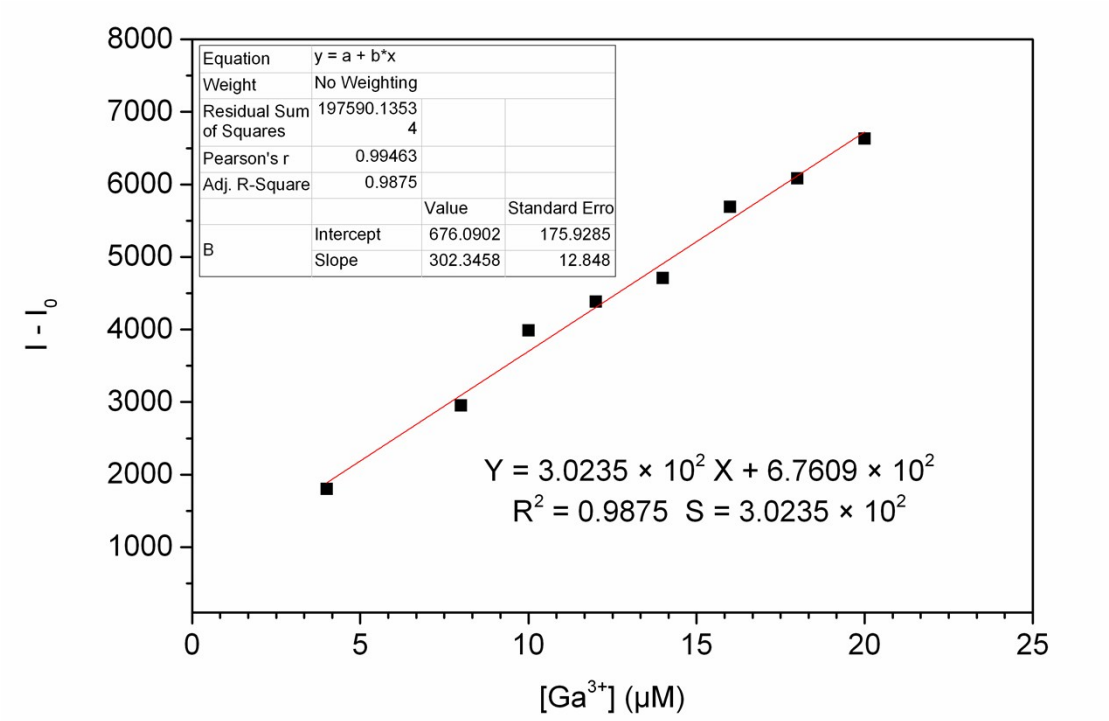

Fig. S21. The fluorescence intensity of **L** (5.0 μM) at 518 nm with addition of linear increase of Ga^{3+} concentration in the range of 4.0 – 20.0 μM. The limit of detection (LOD) of **L** with Ga^{3+} was determined from the following equation: $C_{LOD} = k \times \delta / S$, where k = 3; δ is the standard deviation of the blank solution (0.789); S is the slope of the calibration curve.

The result of the analysis as follows:

Linear Equation: $Y = 3.0235 \times 10^2 X + 6.7609 \times 10^2$ $R^2 = 0.9875$ $S = 3.0235 \times 10^2$

$$\delta = \sqrt{\frac{\sum\left(F_0 - \bar{F_0}\right)^2}{n-1}} = 0.789, n = 10, K = 3$$

$LOD = K \times \delta / S = 3 \times 0.789 / 3.0235 \times 10^2 = 7.83 \times 10^{-3}$ μM

F_0 is the fluorescence intensity at 504 nm of **L**.

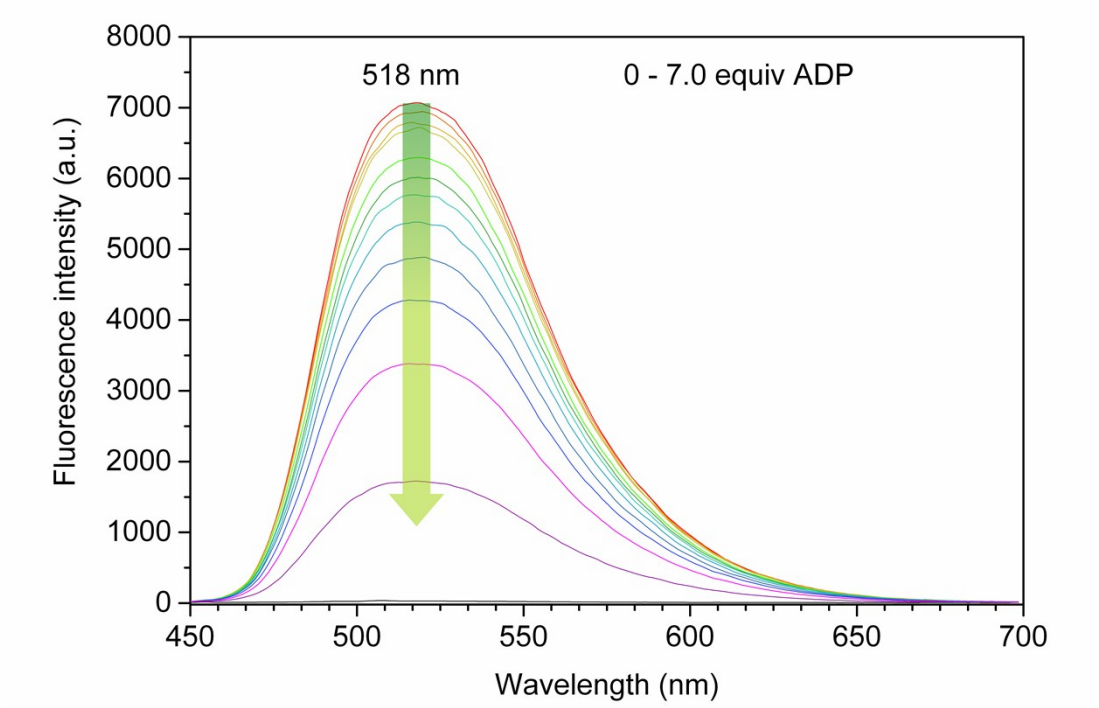

Fig. S22. Fluorescence changes in L-Ga^{3+} complex (1:10, 5.0 μM) upon addition of ADP (0–7.0 equiv.) in DMSO/H_2O (*v*/*v* = 9/1) solution.

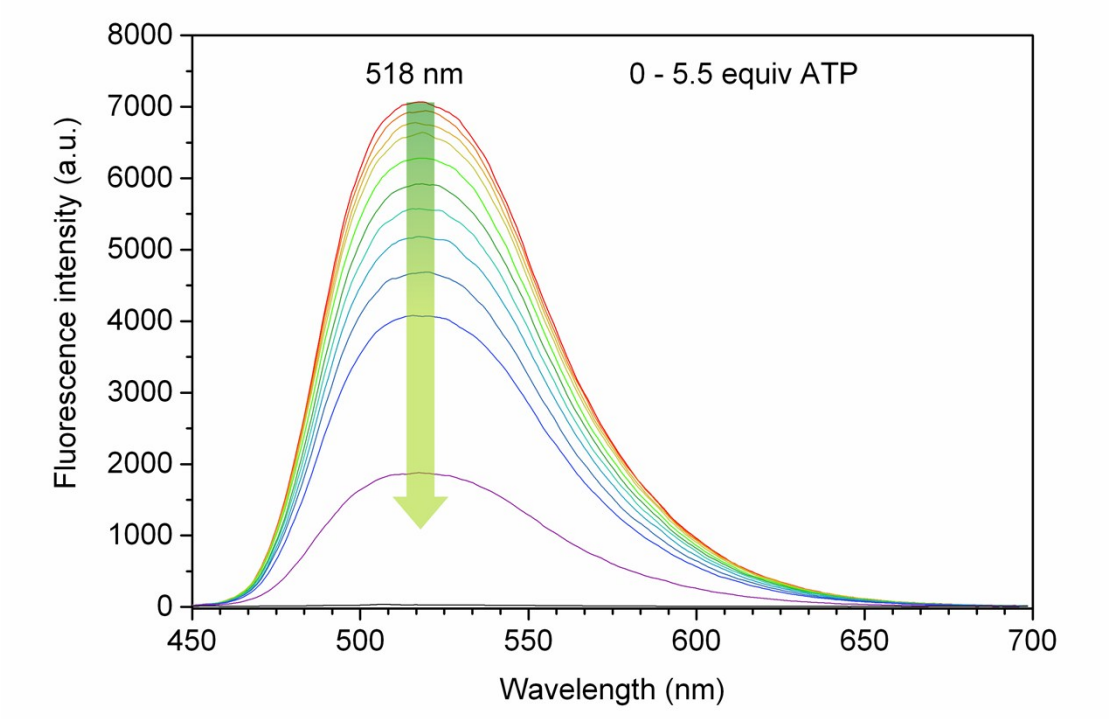

Fig. S23. Fluorescence changes in L-Ga^{3+} complex (1:10, 5.0 μM) upon addition of ATP (0–5.5 equiv.) in DMSO/H_2O (*v*/*v* = 9/1) solution.

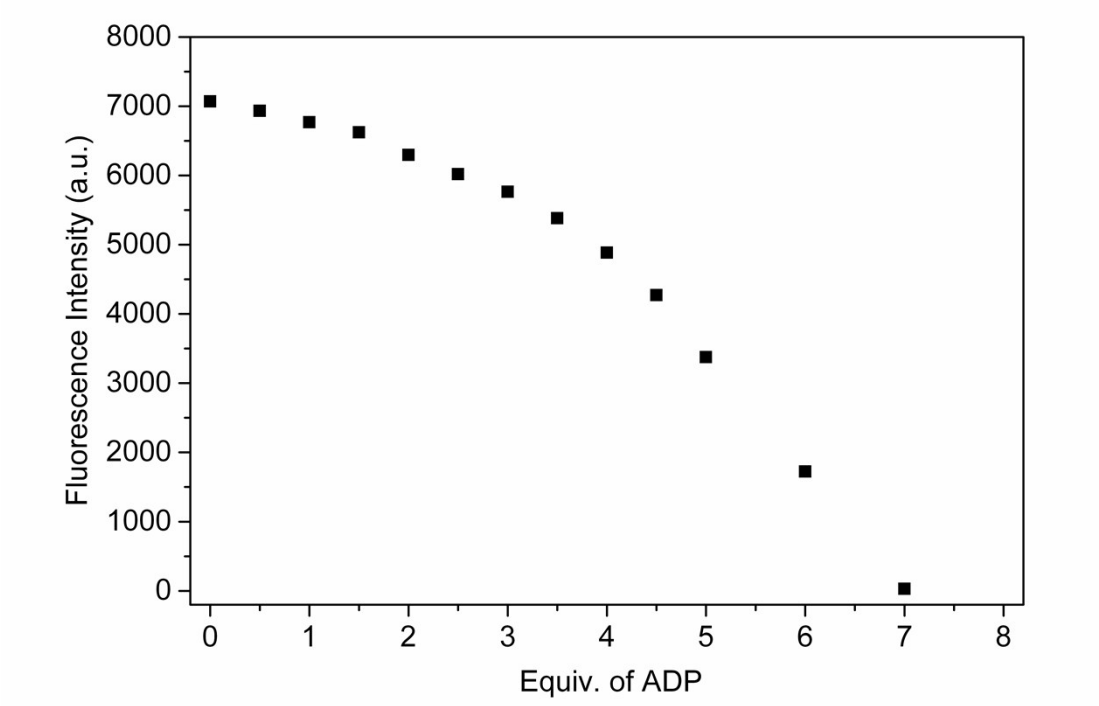

Fig. S24. The dependence of fluorescence emission intensity of L-Ga^{3+} at 518 nm (λ_{ex} = 440 nm) on the amount of ADP added.

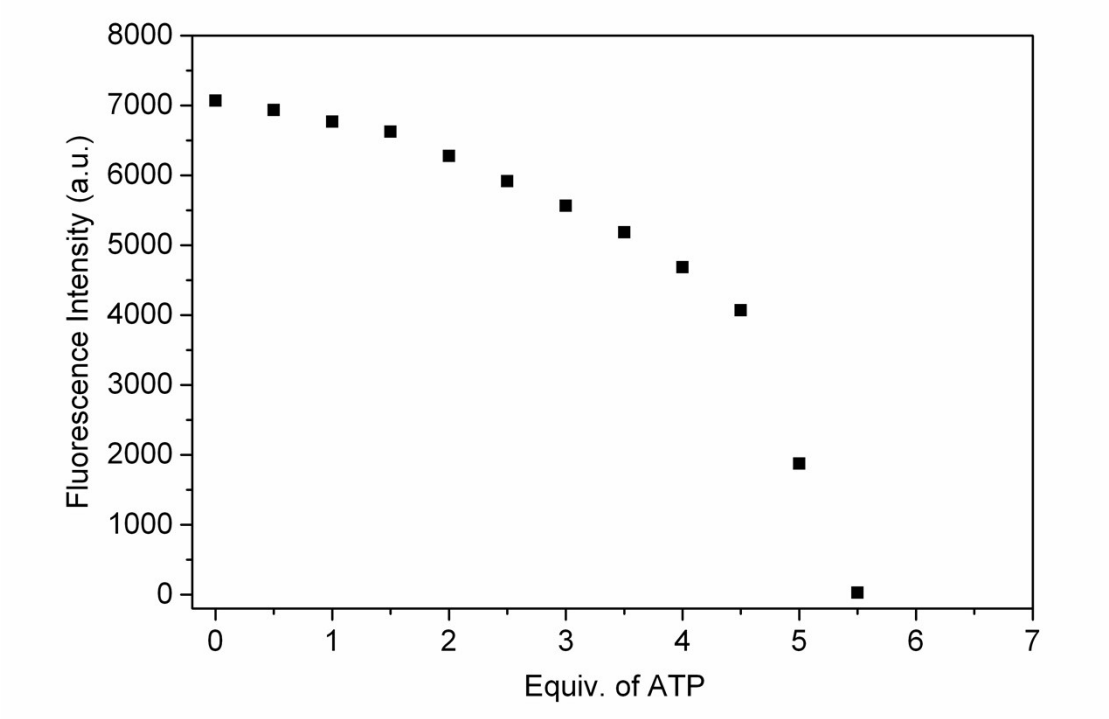

Fig. S25. The dependence of fluorescence emission intensity of L-Ga^{3+} at 518 nm (λ_{ex} = 440 nm) on the amount of ATP added.

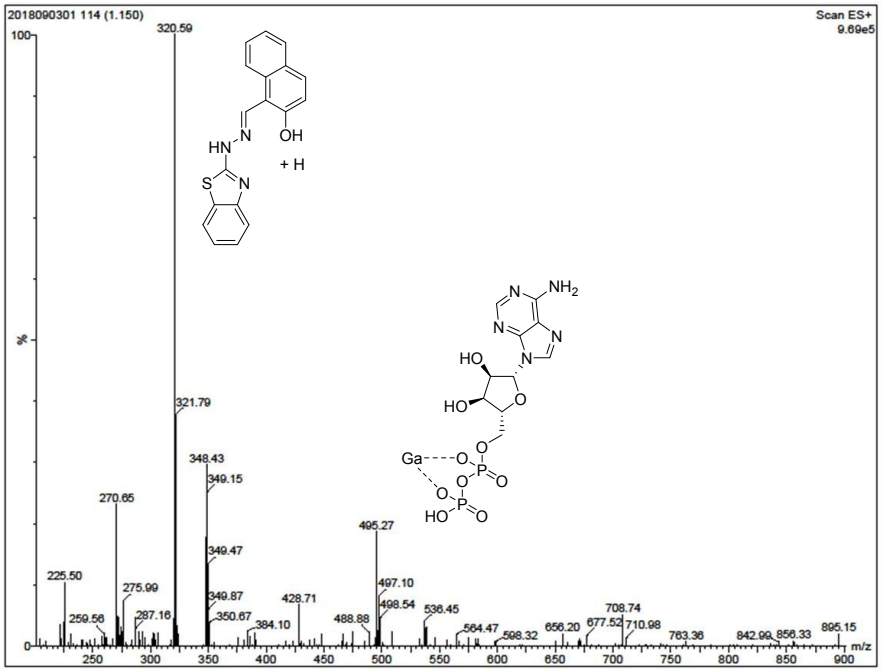

Fig. S26. The ESI-MS spectrum of L-Ga^{3+} upon addition of large excess of ADP in positive mode. ESI-MS (*m*/*z*): 320.59 [**L** + H]$^+$ (Calcd. for $C_{18}H_{14}N_3OS$: 320.09). ESI-MS (*m*/*z*): 495.27 [Ga(ADP)]$^+$ (Calcd. for $C_{10}H_{13}GaN_5O_{10}P_2$: 494.94).

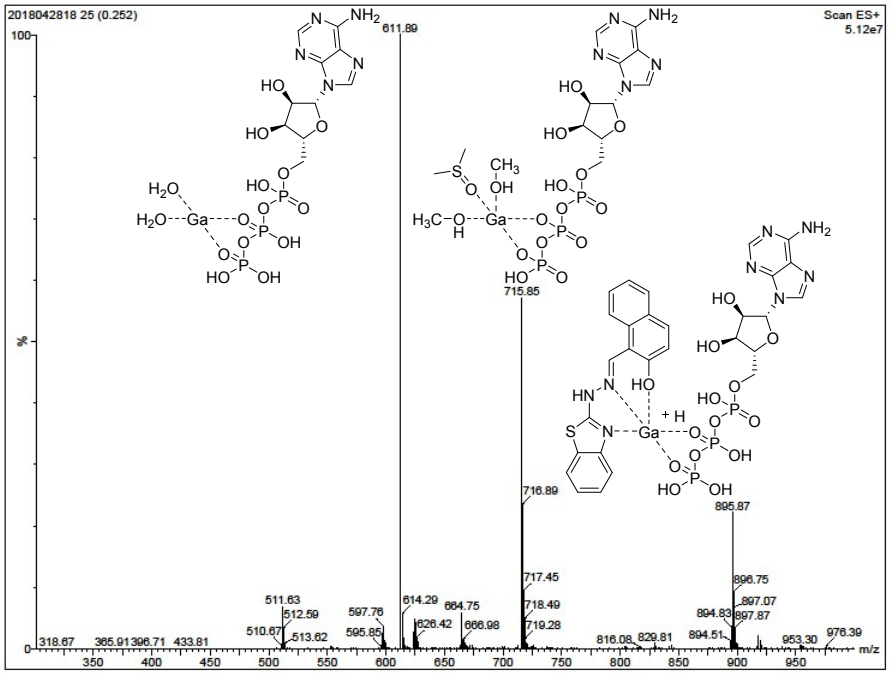

Fig. S27. The ESI-MS spectrum of L-Ga^{3+} upon addition of slight excess of ATP in positive mode. ESI-MS (*m*/*z*): 611.89 [Ga(ATP)(H_2O)]$^+$ (Calcd. for $C_{10}H_{20}GaN_5O_{15}P_3$: 611.94). ESI-MS (*m*/*z*): 715.85 [Ga(ATP)(DMSO)($MeOH$)$_2$ - 2H]$^+$ (Calcd. for $C_{14}H_{28}GaN_5O_{16}P_3S$: 715.97). ESI-MS (*m*/*z*): 896.87 [Ga(NABT)(ATP) + H$^+$]$^+$ (Calcd. for $C_{28}H_{30}GaN_8O_{14}P_3S$: 896.01).

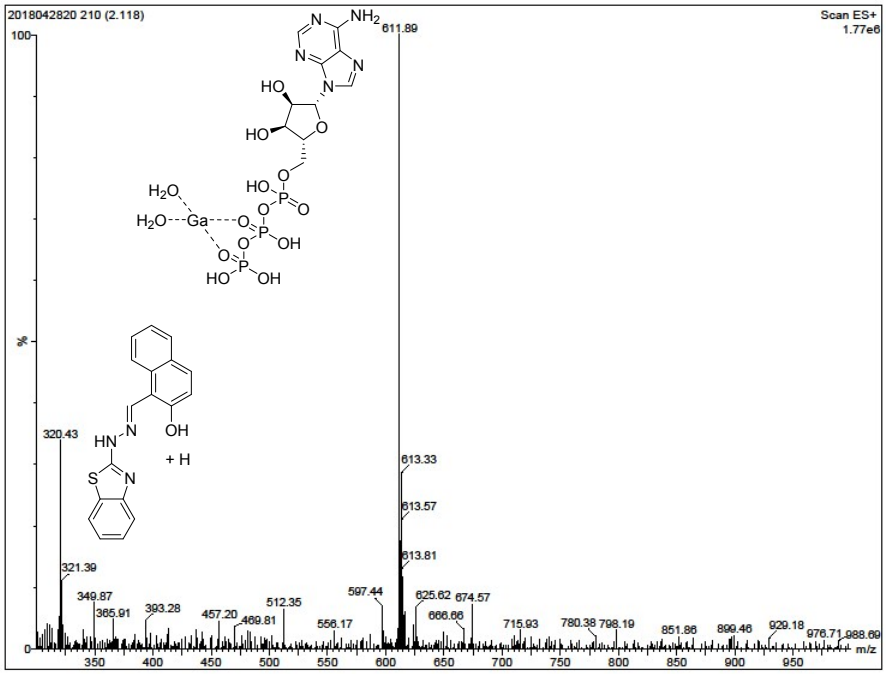

Fig. S28. The ESI-MS spectrum of L-Ga^{3+} upon addition of large excess of ATP in positive mode. ESI-MS (*m*/*z*): 320.43 [**L** + H]$^+$ (Calcd. for $C_{18}H_{14}N_3OS$: 320.09). ESI-MS (*m*/*z*): 611.89 [Ga(ATP)(H_2O)]$^+$ (Calcd. for $C_{10}H_{20}GaN_5O_{15}P_3$: 611.94).

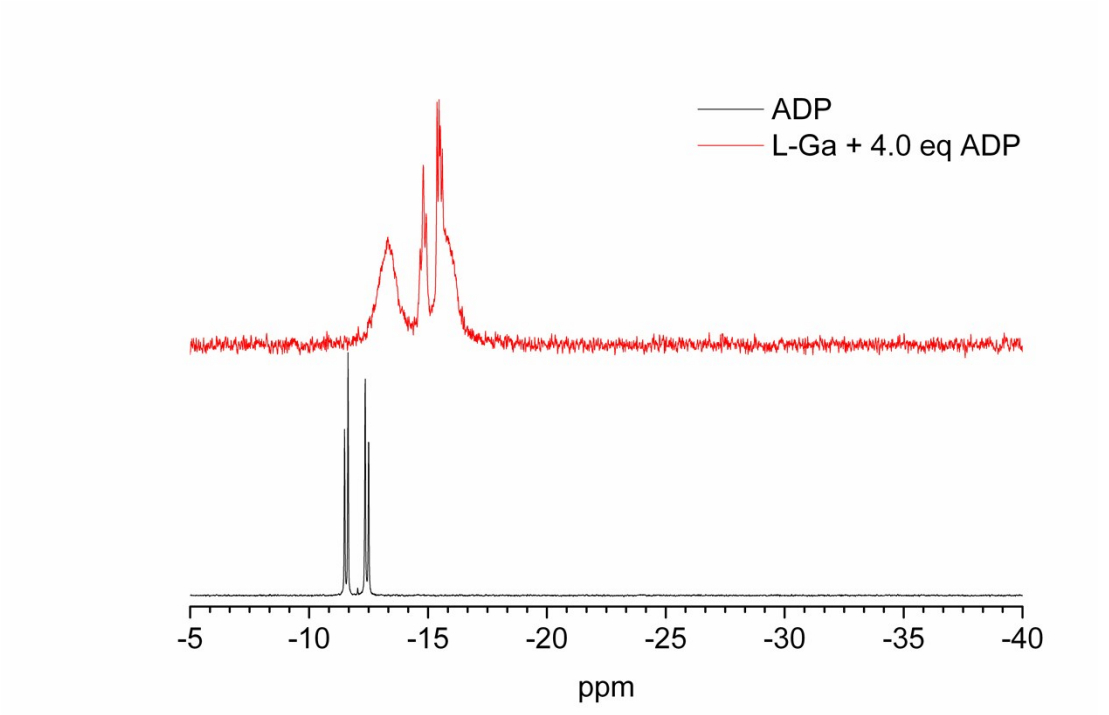

Fig. S29. The ^{31}P NMR spectra of L-Ga^{3+} upon addition of ADP in DMSO-d_6 / D_2O (v/v, 9:1) solution.

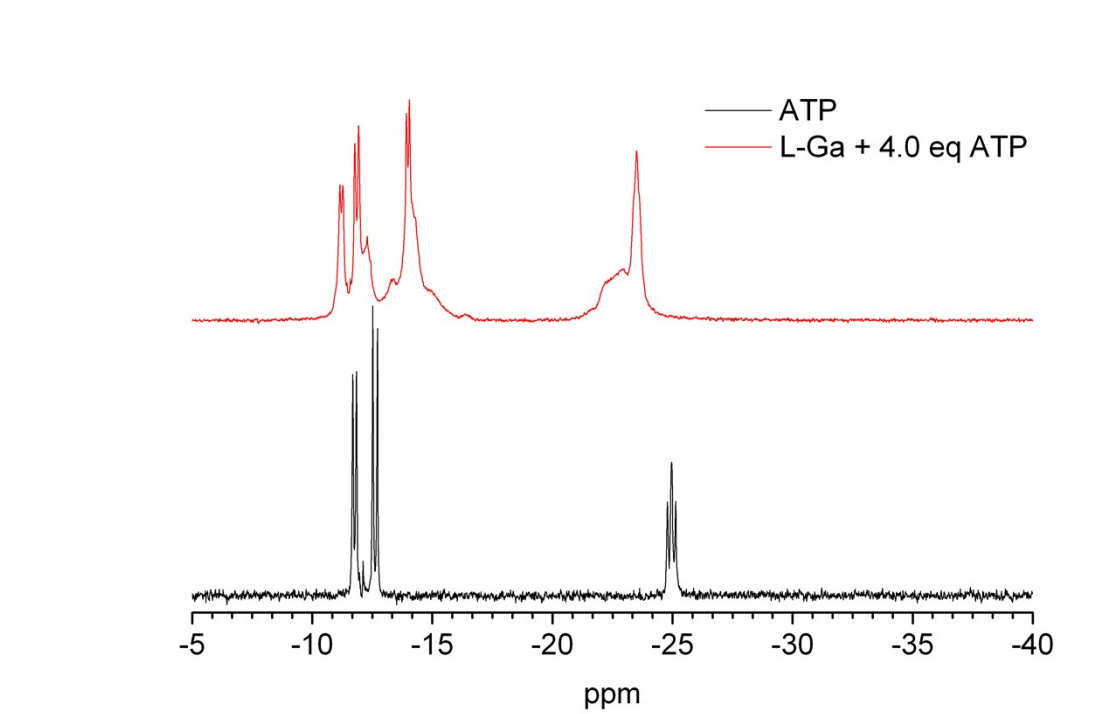

Fig. S30. The ^{31}P NMR spectra of L-Ga^{3+} upon addition of ATP in DMSO-d_6 / D_2O (v/v, 9:1) solution.

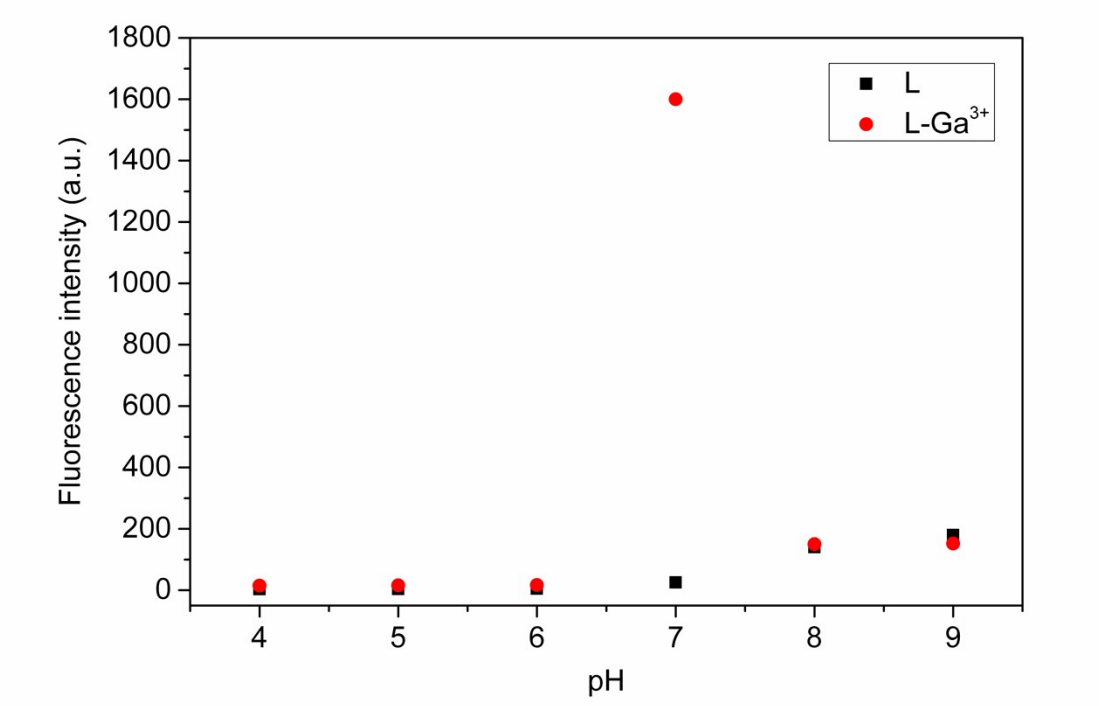

Fig. S31. Fluorescence intensities of probe **L** and L–Ga^{3+} (1:2) complex in DMSO aqueous solutions at different pH values at 518 nm, λ_{ex} = 440 nm.

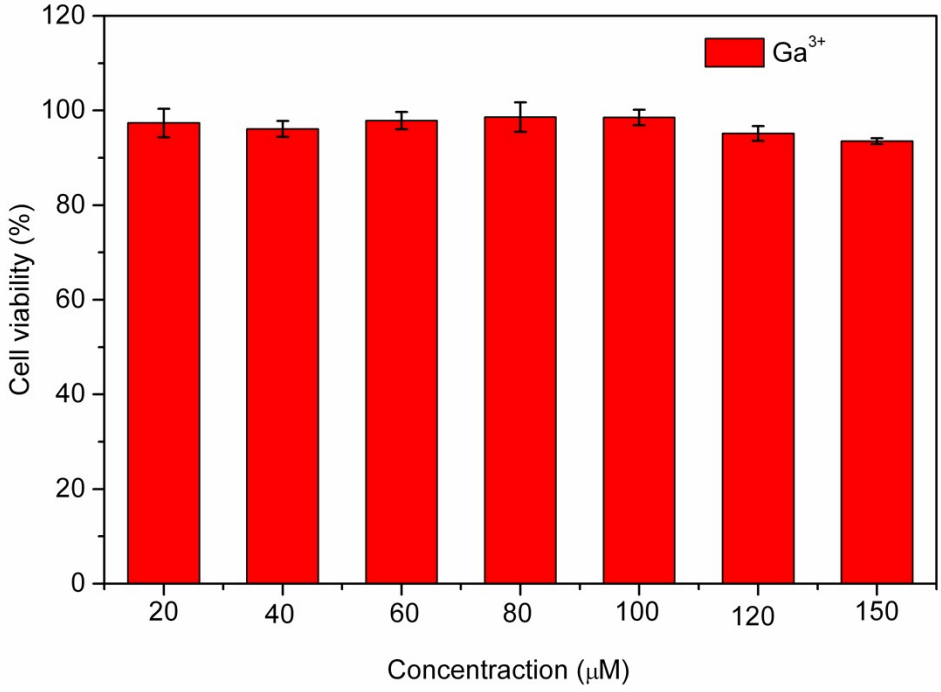

Fig. S32. Cell viability treated with different concentrations of Ga^{3+} (10, 20, 40, 80, 100, 120, and 150 μM) or in 16HBE cells.

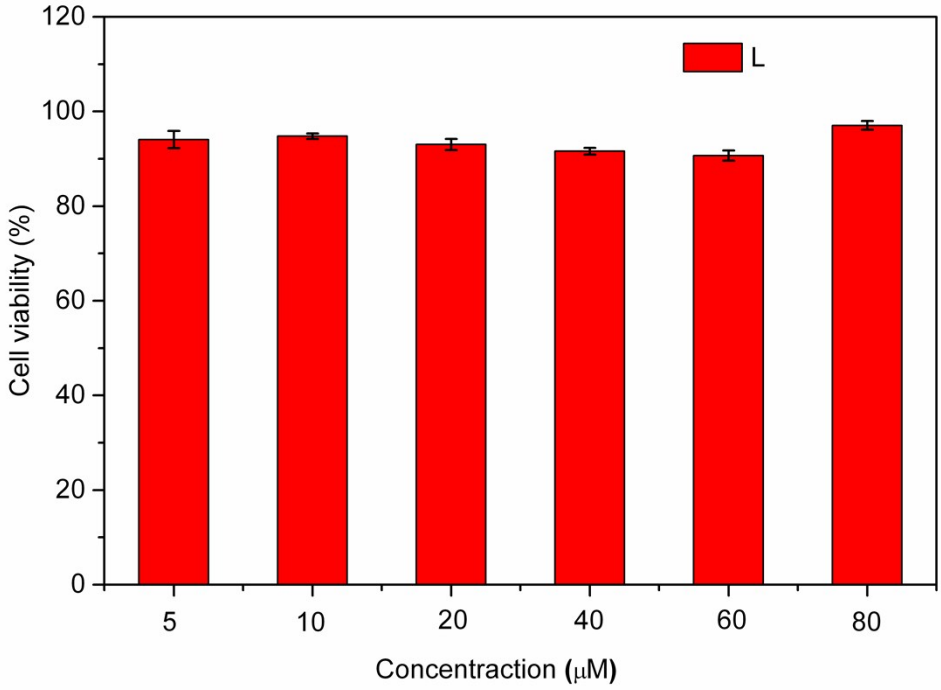

Fig. S33. Cell viability treated with different concentrations of **L** (5, 10, 20, 40, 60, and 80 μM) in 16HBE cells.

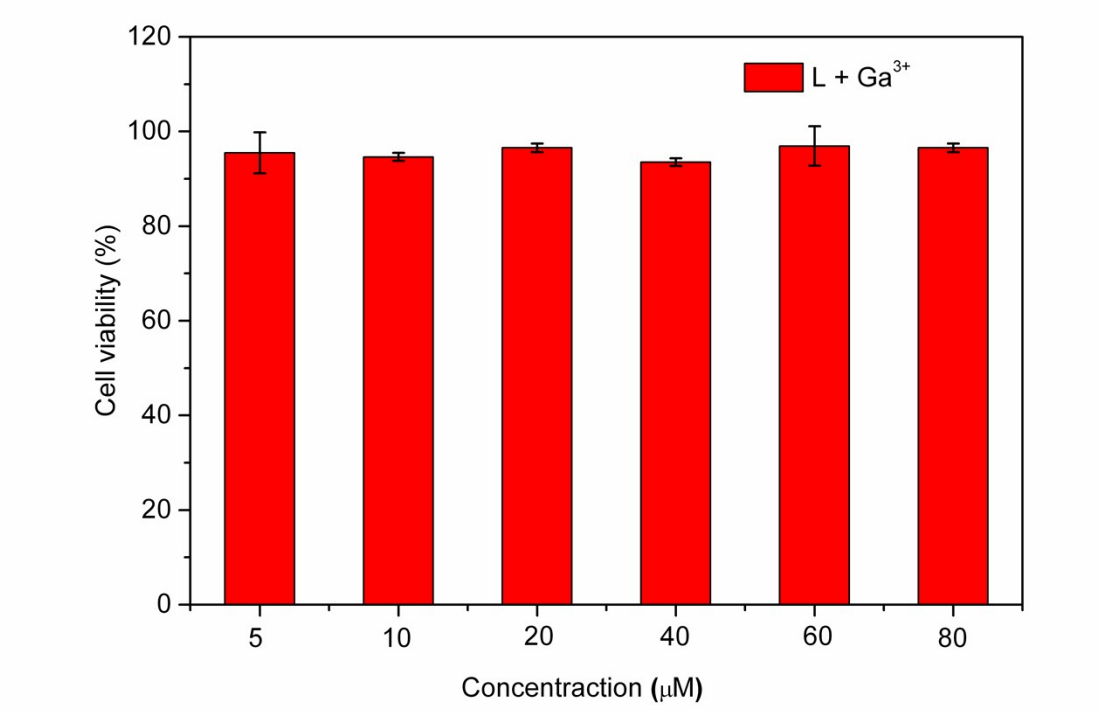

Fig. S34. Cell viability treated with different concentrations of L-Ga^{3+} (5, 10, 20, 40, 60, and 80 μM) in 16HBE cells.

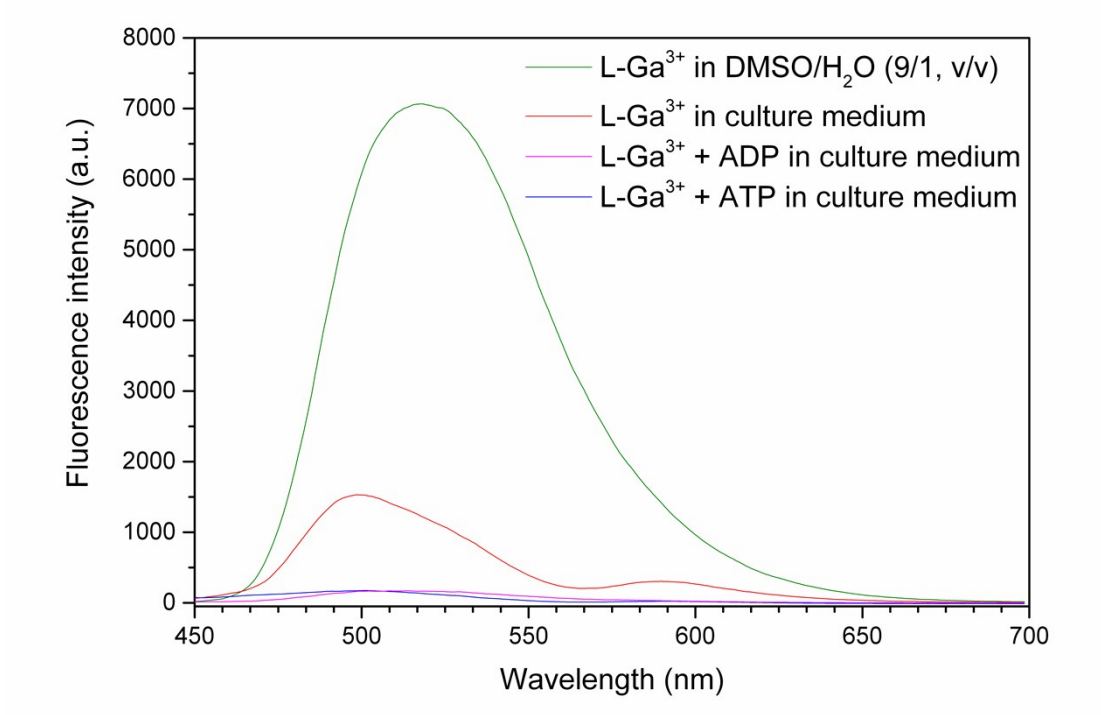

Fig. S35. Fluorescence spectra of L-Ga^{3+}, L-Ga^{3+} + ADP and L-Ga^{3+} + ATP in DMSO/H_2O (v/v, 9:1) and culture medium solution (λ_{ex} = 440 nm).

Table S3. Examples of various Ga^{3+} chemosensors.

Sensor	LOD (μM)	Binding constant (M^{-1})	Interference	Solvent	Ex (nm)	Em (nm)	Reference
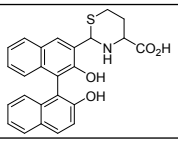	1.54	3.82×10^4	Al^{3+}, In^{3+}	HEPES buffer	330	409	3
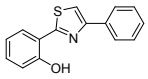	—	6.25×10^4	Al^{3+}, Cu^{2+}	CH_3CN	333	430	4
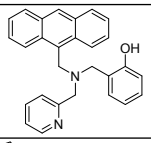	2.4	1.0×10^5	Al^{3+}, Cr^{3+}, In^{3+}, Fe^{3+}	MeOH	364	421	5
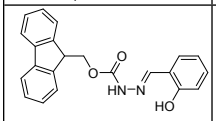	0.01	1.0×10^4	Zn^{2+}	CH_3CN	300	434	6
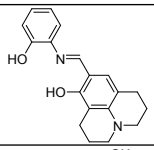	0.1	2.5×10^6	Al^{3+}	MeOH	450	486, 516	7
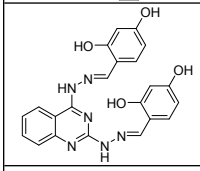	0.05	1.21×10^5	Co^{2+}, Cu^{2+}, Fe^{3+}	EtOH	405	470	8
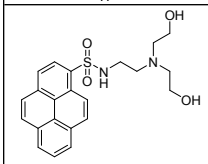	0.01	2.99×10^5	Al^{3+}	HEPES/EtOH = 1/1	340	383	9
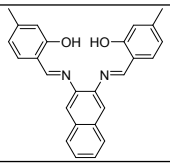	0.012	1.80×10^4	Al^{3+}	acetate buffer/ DMSO = 1/1	422	495	10
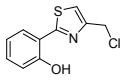	1.0	6.24×10^4	Al^{3+}	CH_3CN	332	431	11
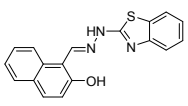	0.00783	5.54×10^4	Al^{3+}, In^{3+}	DMSO/H_2O = 9/1	440	518	This work

Table S4. Crystal data and structure refinement for **L**.

Bond precision: C-C = 0.0029 A		Wavelength=0.71073	
Cell:	a=17.1396(8)	b=4.0692(2)	c=22.0699(15)
	alpha=90	beta=108.746(6)	gamma=90
Temperature:	180 K		
	Calculated	Reported	
Volume	1457.60(15)	1457.60(15)	
Space group	P 21/n	P 21/n	
Hall group	-P 2yn	-P 2yn	
Moiety formula	C18 H13 N3 O S	?	
Sum formula	C18 H13 N3 O S	C18 H13 N3 O S	
Mr	319.37	319.37	
Dx,g cm-3	1.455	1.455	
Z	4	4	
Mu (mm-1)	0.230	0.230	
F000	664.0	664.0	
F000’	664.72		
h,k,lmax	22,5,28	22,5,28	
Nref	3356	3346	
Tmin,Tmax	0.959,0.989	0.301,1.000	
Tmin’	0.891		
Correction method= # Reported T Limits: Tmin=0.301 Tmax=1.000			
AbsCorr = MULTI-SCAN			
Data completeness= 0.997		Theta(max)= 27.480	
R(reflections)= 0.0463(2591)		wR2(reflections)= 0.1224(3346)	
S = 1.031		Npar= 212	

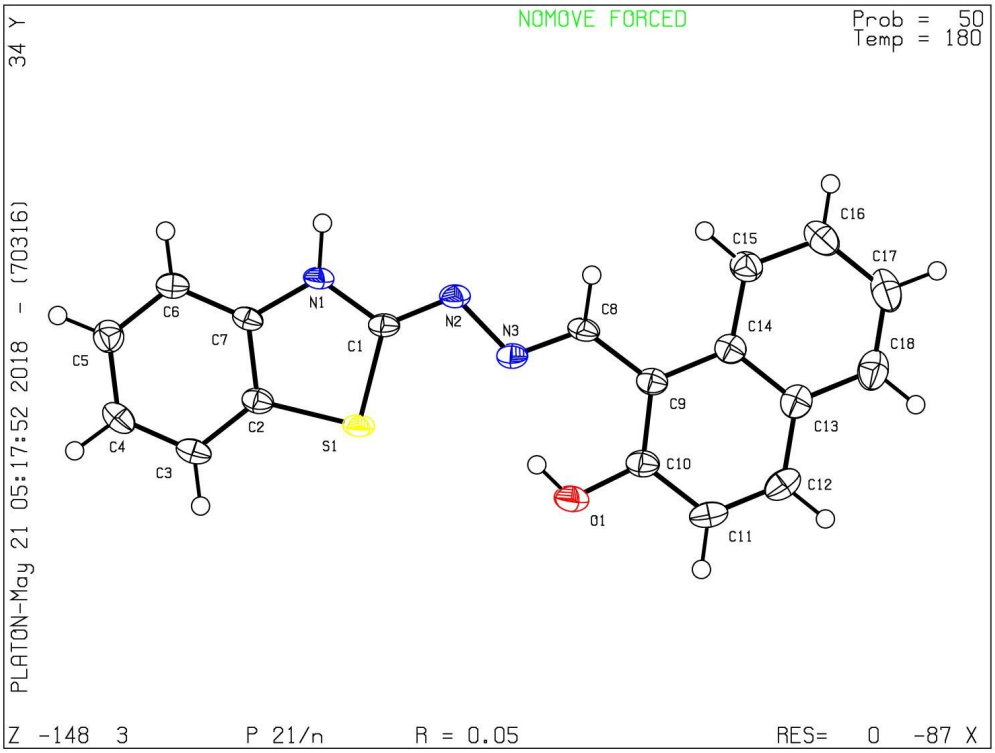

Fig. S36. The single crystal structure of **L**.

Table S5. Bond lengths [Å] for **L**.

Number	Atom1	Atom2	Length	Number	Atom1	Atom2	Length
1	S1	C1	1.753(2)	21	C8	H8	0.929
2	S1	C2	1.757(2)	22	C8	C9	1.452(2)
3	O1	H1A	0.82	23	C9	C10	1.392(2)
4	O1	C10	1.344(3)	24	C9	C14	1.439(3)
5	N1	H1	0.93(1)	25	C10	C11	1.410(2)
6	N1	C1	1.360(2)	26	C11	H11	0.929
7	N1	C7	1.383(3)	27	C11	C12	1.356(4)
8	N2	N3	1.397(2)	28	C12	H12	0.93
9	N2	C1	1.301(3)	29	C12	C13	1.414(3)
10	N3	C8	1.288(3)	30	C13	C14	1.429(3)
11	C2	C3	1.382(3)	31	C13	C18	1.407(4)
12	C2	C7	1.396(2)	32	C14	C15	1.413(3)
13	C3	H3	0.93	33	C15	H15	0.93
14	C3	C4	1.386(3)	34	C15	C16	1.367(3)
15	C4	H4	0.931	35	C16	H16	0.93
16	C4	C5	1.387(2)	36	C16	C17	1.404(3)
17	C5	H5	0.93	37	C17	H17	0.93
18	C5	C6	1.383(3)	38	C17	C18	1.361(3)
19	C6	H6	0.929	39	C18	H18	0.93
20	C6	C7	1.388(3)				

Table S6. Bond angles [°] for **L**.

Number	Atom1	Atom2	Atom3	Angle	Number	Atom1	Atom2	Atom3	Angle
1	C1	S1	C2	90.55(8)	32	C8	C9	C10	120.5(2)
2	H1A	O1	C10	109.5	33	C8	C9	C14	120.4(2)
3	H1	N1	C1	122(1)	34	C10	C9	C14	119.1(2)
4	H1	N1	C7	124(1)	35	O1	C10	C9	122.7(2)
5	C1	N1	C7	114.7(1)	36	O1	C10	C11	116.3(2)
6	N3	N2	C1	111.5(1)	37	C9	C10	C11	121.0(2)
7	N2	N3	C8	113.7(1)	38	C10	C11	H11	120
8	S1	C1	N1	111.2(1)	39	C10	C11	C12	120.2(2)
9	S1	C1	N2	126.7(1)	40	H11	C11	C12	119.8
10	N1	C1	N2	122.1(2)	41	C11	C12	H12	119.1
11	S1	C2	C3	128.0(1)	42	C11	C12	C13	121.8(2)
12	S1	C2	C7	110.6(1)	43	H12	C12	C13	119.1
13	C3	C2	C7	121.3(2)	44	C12	C13	C14	118.8(2)
14	C2	C3	H3	121.1	45	C12	C13	C18	121.7(2)
15	C2	C3	C4	117.9(2)	46	C14	C13	C18	119.4(2)
16	H3	C3	C4	121	47	C9	C14	C13	119.1(2)
17	C3	C4	H4	119.5	48	C9	C14	C15	123.5(2)
18	C3	C4	C5	121.0(2)	49	C13	C14	C15	117.4(2)
19	H4	C4	C5	119.5	50	C14	C15	H15	119.2
20	C4	C5	H5	119.3	51	C14	C15	C16	121.5(2)
21	C4	C5	C6	121.2(2)	52	H15	C15	C16	119.3
22	H5	C5	C6	119.5	53	C15	C16	H16	119.6
23	C5	C6	H6	120.9	54	C15	C16	C17	120.7(2)
24	C5	C6	C7	118.1(2)	55	H16	C16	C17	119.6
25	H6	C6	C7	121	56	C16	C17	H17	120.3
26	N1	C7	C2	112.9(2)	57	C16	C17	C18	119.4(2)
27	N1	C7	C6	126.7(2)	58	H17	C17	C18	120.3
28	C2	C7	C6	120.4(2)	59	C13	C18	C17	121.6(2)
29	N3	C8	H8	118.6	60	C13	C18	H18	119.2
30	N3	C8	C9	122.8(2)	61	C17	C18	H18	119.2
31	H8	C8	C9	118.6					

References:

1. A. Gogoi, S. Samanta and G. Das, *Sens. Actuators, B*, 2014, **202**, 788−794.
2. N. Xiao, L. Xie, X. Zhi and C.−J. Fang, *Inorg. Chem. Commun.*, 2018, **89**, 13−17.
3. Y.-W. Wang, S.-B. Liu, W.-J. Ling and Y. Peng, *Chem. Commun.*, 2016, **52**, 827-830.
4. B.-Y. Kim, H.-S. Kim and A. Helal, *Sens. Actuators, B*, 2015, **206**, 430-434.
5. H. Kim, K. B. Kim, E. J. Song, I. H. Hwang, J. Y. Noh, P.-G. Kim, K.-D. Jeong and C. Kim, *Inorg. Chem. Commun.*, 2013, **36**, 72-76.
6. S. Y. Lee, K. H. Bok, T. G. Jo, S. Y. Kim and C. Kim, *Inorg. Chim. Acta*, 2017, **461**, 127-135.
7. J. Y. Noh, S. Kim, I. H. Hwang, G. Y. Lee, J. Kang, S. H. Kim, J. Min, S. Park, C. Kim and J. Kim, *Dyes Pigm.*, 2013, **99**, 1016-1021.
8. J. Kimura, H. Yamada, H. Ogura, T. Yajima and T. Fukushima, *Anal. Chim. Acta*, 2009, **635**, 207-213.
9. A. Kumar and P. S. Chae, *Anal. Chim. Acta*, 2017, **958**, 38-50.
10. Z. Zeng, R. Ma, C. Liu, Y. Xu, H. Li, F. Liu and S. Sun, *Sens. Actuators, B*, 2017, **250**, 267-273.
11. C. Lim, M. An, H. Seo, J. H. Huh, A. Pandith, A. Helal and H.-S. Kim, *Sens. Actuators, B*, 2017, **241**, 789-799.